

Review

Amino acid-containing reduced Schiff bases as the building blocks for metallasupramolecular structures

Rakesh Ganguly, Bellam Sreenivasulu, Jagadese J. Vittal*

Department of Chemistry, Science Drive 3, National University of Singapore, Singapore 117543, Singapore

Received 14 May 2007; accepted 5 January 2008

Available online 15 January 2008

Contents

1. Introduction	1028
2. Reduced Schiff base ligands	1028
3. Metallasupramolecular structures derived from <i>N</i> -(2-hydroxybenzyl)-amino acid ligands	1028
3.1. Type 1: Monomer and dimer as the building blocks	1029
3.1.1. Metal complexes associated with supramolecular isomerism	1032
3.1.2. Solid state supramolecular structural transformations induced by thermal dehydration	1034
3.1.3. 3D coordination polymer with star-like cavity	1036
3.1.4. Hydrogen-bonded 1D coordination polymers forming supramolecular networks	1036
3.1.5. Schiff base <i>versus</i> reduced Schiff base ligands: A case study	1037
3.1.6. Helical staircase coordination polymer hosting helical water chain	1039
3.1.7. Influence of cation on molecular assembly	1040
3.2. Type 2: Metal aggregates and oligomeric building blocks	1040
4. Metallasupramolecular structures derived from <i>N</i> -(2-pyridyl)-amino acid ligands	1041
4.1. Influence of cation and pH on metallacrown cations	1041
4.2. Influence of the nature of reactants on metallacrown cations	1042
4.3. Influence of anions on 1D polymers	1043
4.4. Solvent dependent supramolecular assembly	1044
4.5. Formation of cubane-like aggregate	1045
5. Ternary complexes	1045
5.1. Complexes with 1,10-phenanthroline as co-ligand	1045
5.2. Complexes with other co-ligands	1048
6. Conclusions	1049
Acknowledgements	1049
References	1049

Abstract

Metal coordination compounds derived from several closely related yet different multidentate reduced Schiff base ligands (obtained by reducing the C=N bond in the Schiff bases formed by the condensation of aldehyde and various natural/unnatural amino acids) are discussed in terms of their mode of binding and coordination to supramolecular network structures. These multidentate ligands have flexible backbone with hydrogen bond donors and acceptors, and readily form metal complexes and coordination polymers with metal ions such as Cu(II), Zn(II), and Ni(II). Various solid-state metallasupramolecular network structures are delineated ranging from hydrogen-bonded linear polymers and helical coordination polymers, 2D sheets to 3D network architectures constructed *via* N–H···O, C=O···H–O_{solvent}, O–H···O, N–H···O=C hydrogen bonds and C=O···π, C–H···π, and π···π stacking interactions. This review gives an account of the observed structural diversity in relation to the role of different donors and acceptors, aqua ligand and solvents, nature of the ligands and metal ions, coordination geometry around the metal ions and counter

* Corresponding author. Tel.: +65 6516 2975; fax: +65 6779 1691.
E-mail address: chmjv@nus.edu.sg (J.J. Vittal).

ions besides the experimental conditions such as temperature, pH, etc. in directing the formation of supramolecular structures in the solid state. Some other related and interesting examples from the literature are also mentioned.

© 2008 Elsevier B.V. All rights reserved.

Keywords: Reduced Schiff base; Amino acid; Hydrogen bond; Coordination polymers; Thermal dehydration reactions; Helical structures; Self-assembly

1. Introduction

In the past decades, significant progress has been achieved in understanding the chemistry of transition metal complexes with Schiff base ligands composed of salicylaldehyde or analogues and α -amino acids [1]. Most of the model studies of such metal complexes have focused upon various binding modes of these ligands and the X-ray crystal structures of complexes revealed that the Schiff base ligands mainly act as tridentate moiety, coordinating through the phenolato oxygen, imine nitrogen, and carboxylate oxygen. The metal complexes containing Schiff bases are the most fundamental chelating systems in coordination chemistry [2]. Casella and Gullotti have shown that Schiff bases formed by amino acids with non-polar side chains and 2-formylpyridine were unstable with Zn(II) and Cu(II), and only imines of histidine or its methyl ester could be isolated in reasonable purity [3]. The problems with ligand instability can be overcome by reducing the C=N bond of the Schiff base to give an amine, also known as *Mannich base*, and the reduced Schiff bases are expected to generate much more interesting coordination chemistry due to the conformationally flexible backbone. In this connection, several copper complexes with reduced Schiff base ligands between salicylaldehyde and amino acids were explored to serve as models for the intermediate species in biological racemization and transamination reactions [4].

The reduced Schiff base ligands, *N*-(2-hydroxybenzyl)-amino acids and *N*-(2-pyridylmethyl)-amino acids derived from various substituted salicylaldehydes and 2-pyridinealdehyde respectively, form a class of multidentate ligands with flexible backbone useful in constructing interesting supramolecular structures. The successful construction of a variety of coordination polymeric structures mainly depends on the lability of metal–ligand bonds in solution which allows for the breaking and making of new bonds in solution. On the other hand, the role of different donors and acceptors, aqua ligand and solvents, nature of the ligands and metal ions, etc., besides the experimental and crystallization conditions determines the type of the complexes formed in the solid state particularly when there are many species in equilibrium in solution. The direction of alignment of these oligomeric species in a particular fashion can be controlled to form interesting supramolecular structures by incorporating hydrogen bond donors and acceptors at the backbone of the ligands apart from the hydrogen bonding possibilities from the lattice water, solvents and aqua ligands. In this context, this review summarizes metal coordination chemistry of natural/unnatural amino-acid based reduced Schiff base ligands and, the structural diversity and the phenomena associated with several solid-state metallasupramolecular network structures of the corresponding metal complexes. The role of various weaker interactions ($\text{N-H} \cdots \text{O}$, $\text{C=O} \cdots \text{H-O}_{\text{solvent}}$, $\text{O-H} \cdots \text{O}$,

$\text{N-H} \cdots \text{O}=\text{C}$, hydrogen bonds and $\text{C=O} \cdots \pi$, $\text{C-H} \cdots \pi$, and $\pi \cdots \pi$ stacking interactions) is also discussed.

2. Reduced Schiff base ligands

The reduced Schiff base ligands discussed in this review broadly fall into two groups *viz.* *N*-(2-hydroxybenzyl)-amino acids (Fig. 1A) and *N*-(2-pyridylmethyl)-amino acids (Fig. 1B). These ligands are obtained by reducing the C=N bond in the Schiff base formed by the simple condensation of aldehydes with amino acids. Compared to the Schiff bases, the corresponding reduced Schiff bases are expected to be more stable and adaptable to form conformationally flexible 5- or 6-membered rings upon complexation as they are not constrained to be planar. The hydrogen atom on the secondary amine produced after the reduction of the azomethine ($-\text{CH}=\text{N}-$) fragment of the Schiff base is expected to be significantly acidic due to metal ion coordination to the amine N-atom. Hence this N–H proton can participate in intermolecular hydrogen-bonding interactions ($\text{N-H} \cdots \text{O}$), with the carboxylate oxygen ($\text{C=O} \cdots \text{H-N}$) in the amino acid side arm, required for the supramolecular self-assembly of the building blocks. Also, the presence of chiral amino acid side arm in the ligands helps to induce the chirality in the supramolecular connectivity. Another major advantage of these ligands is the effective involvement of carbonyl oxygen donor from the simple amino acid side arm in connecting the neighboring metal centers *via* intermolecular coordination bonds to generate interesting 2D and 3D coordination network structures. Further, these ligands can also afford the choice of coordination environments that determine the nature of metal ions that can be bound within the closest proximity resulting in the dinuclear complexes.

Various supramolecular structures of transition metal complexes obtained from these ligands are discussed in the following sections.

3. Metallasupramolecular structures derived from *N*-(2-hydroxybenzyl)-amino acid ligands

During the self-assembly process resulting in the formation of hydrogen-bonded metal complexes or coordination polymers, there is an advantage that both coordination bonds and, perhaps, more predictable hydrogen bonds can be utilized in constructing supramolecular structures. Furthermore, incorporation of hydrogen bond donors and acceptors at the backbone of the ligands will assist in directing the alignment of coordination polymers in a desired fashion to form interesting multidimensional network structures. In this context, a variety of multidentate reduced Schiff base ligands, *N*-(2-hydroxybenzyl)-amino acids have been employed in the construction of various hydrogen-bonded metal coordination polymeric struc-

tures. The following sections deal with the formation of various supramolecular structures from different monomeric, dimeric and oligomeric units of metal complexes as building blocks and the nature of reactants, experimental and crystallization conditions. The role of strong $\text{N-H} \cdots \text{O}$ and $\text{O-H} \cdots \text{O}$ hydrogen bonds involving aqua ligands, N-H and carboxylate groups is also discussed.

3.1. Type 1: Monomer and dimer as the building blocks

N-(2-hydroxybenzyl)-amino acid ligands are known to give a variety of complexes depending on the metal to ligand ratio. Of

these 1:1 ratio mostly gives dinuclear complexes in which the two-phenolate oxygen atoms bridge two metal ions to furnish a M_2O_2 core. Apparently simple looking monomers and dimers can give rise to very interesting supramolecular architectures in the solid-state owing to the hydrogen bonding as exemplified in the following sections.

Reaction of the Li salt of *D, L*- H_2Sala with $\text{Cu}(\text{OAc})_2 \cdot \text{H}_2\text{O}$ gives a centrosymmetric binuclear compound, $[\text{Cu}_2(\text{D, L-Sala})_2(\text{H}_2\text{O})_2] \cdot 2\text{H}_2\text{O}$ (1) with both *D* and *L* ligands coordinated to the $\text{Cu}(\text{II})$ centers in a *mer* fashion through bridging phenolate, carbonyl oxygen and the amine nitrogen atoms [5]. The apical coordination sites are occupied by water molecules in

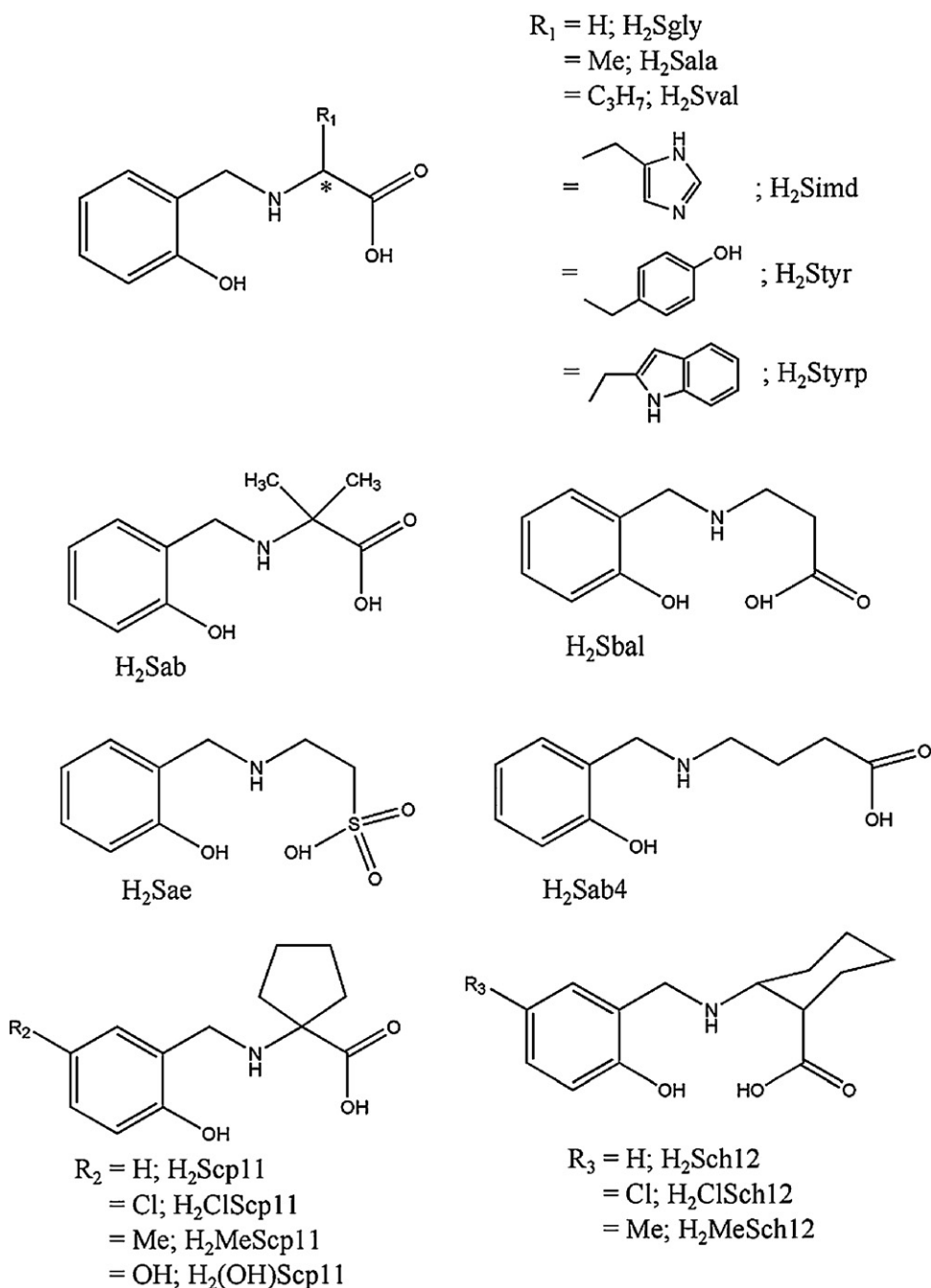


Fig. 1. Reduced Schiff base ligands (A) *N*-(2-hydroxybenzyl)-amino acids and (B) *N*-(2-pyridylmethyl)-amino acids.

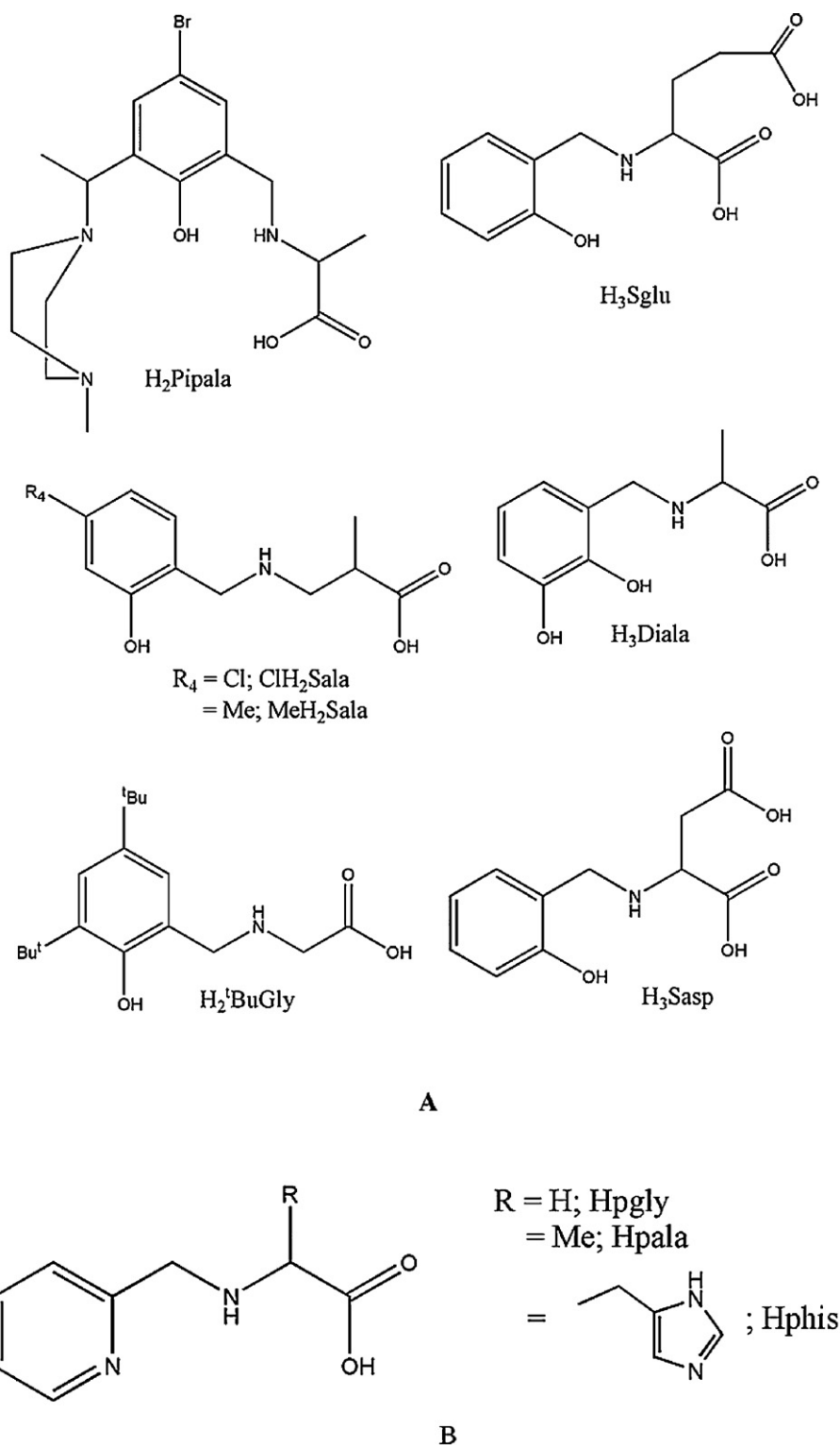


Fig. 1. (Continued).

trans fashion (as shown in Fig. 2a) which is further assisted by complementary N–H···O bonds as well as O–H···O=C hydrogen bonds. This leads to 1D hydrogen-bonded polymers. The two lattice water molecules, two aqua ligands and two carbonyl oxygen atoms also form strong O–H···O bonds to generate

a 16-membered ring, creating 2D hydrogen-bonded sheets as displayed in Fig. 2b. Similar coordination behavior has been observed in a number of Cu(II) complexes of these amino acid derivatives, but there are minor variations due to coordination at the axial positions.

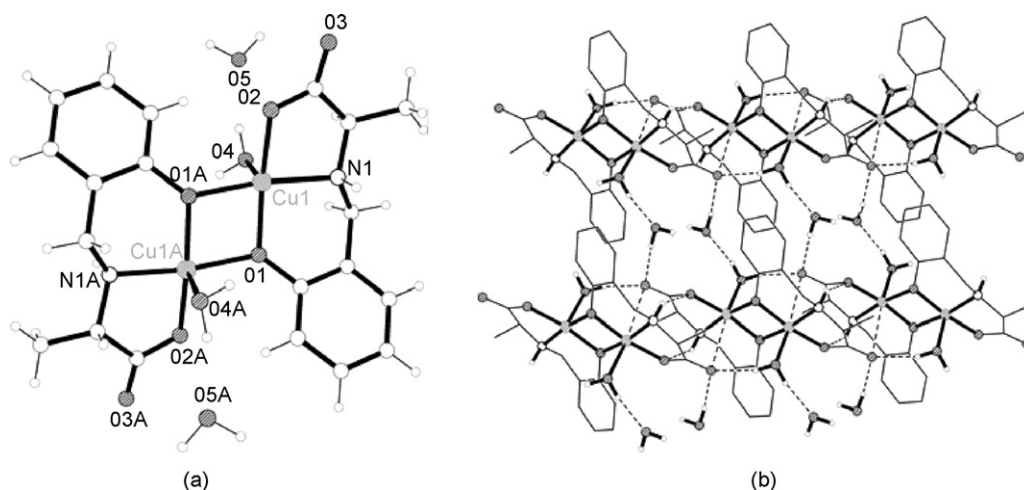


Fig. 2. (a) Ball and stick diagram of **1** showing the coordination environment. (b) A portion of the hydrogen-bonded sheet structure formed by **1**.

For example, the packing in the centrosymmetric dimer $[\text{Cu}_2(\text{Sab})_2(\text{H}_2\text{O})_2]$ (**2**) is similar to that of **1** [5]. The dimer is slip-stacked through weak $\text{Cu} \cdots \text{O}=\text{C}$ bonds complemented by $\text{O}-\text{H} \cdots \text{O}$ hydrogen bonds to form 1D coordination polymer. The amine H atom does not participate in the hydrogen bonding with carboxylate O atom of carboxylate group. In the absence of two lattice water molecules, unlike **1**, these hydrogen-bonded polymers interact with adjacent strands through carbonyl oxygen and hydrogen atoms of the aqua ligand to form 2D hydrogen-bonded sheets as shown below in Fig. 3.

On the other hand, in $[\text{Cu}_2(\text{Styr})_2(\text{H}_2\text{O})] \cdot 2\text{H}_2\text{O}$ (**3**) one Cu(II) center has an aqua ligand in the axial position and axial site in the second Cu(II) is occupied by the carboxylate oxygen from the

neighboring molecule to form a helical coordination polymer as shown in Fig. 4 [5]. The coordination geometry is very similar to **1** but the helical conformation is induced by the chiral ligand with bulky substitution. The coordination polymers are further supported by $\text{O}-\text{H} \cdots \text{O}$ and $\text{N}-\text{H} \cdots \text{O}$ hydrogen bonds in the crystal structure.

The structure of $[\text{Cu}_2(\text{Stryp})_2(\text{H}_2\text{O})]$ (**4**) is similar to that of **3** obtained with a chiral H_2Stryp ligand in terms of the geometry at the metal centers, connectivity, and conformation of the 1D helical coordination polymers [5]. But the crystal packing is slightly different in **4** as there is no lattice water in **4** unlike **3** and hence there is no contribution from the hydrogen bonding from lattice water.

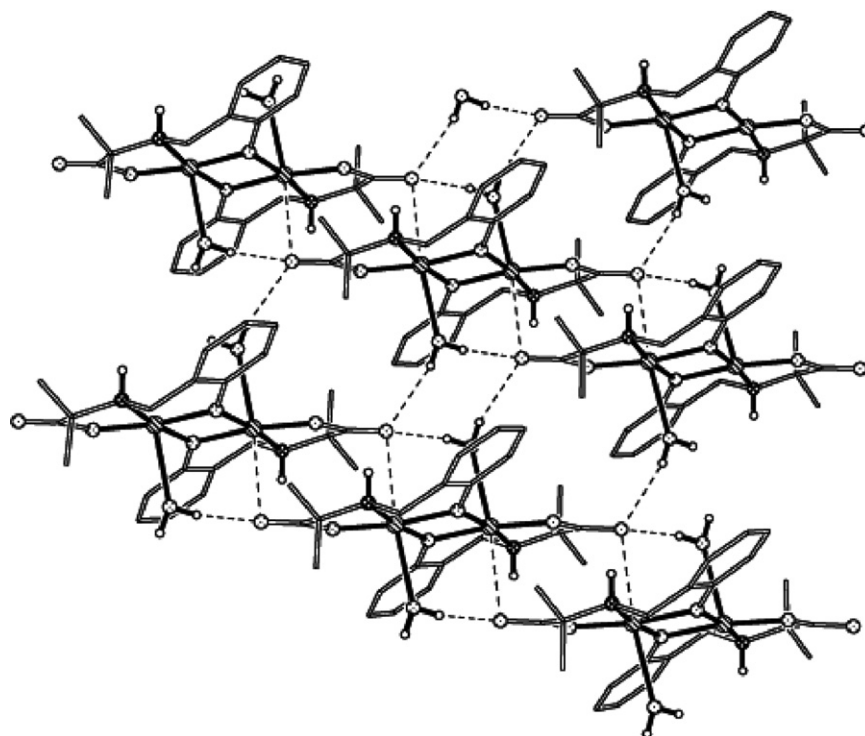
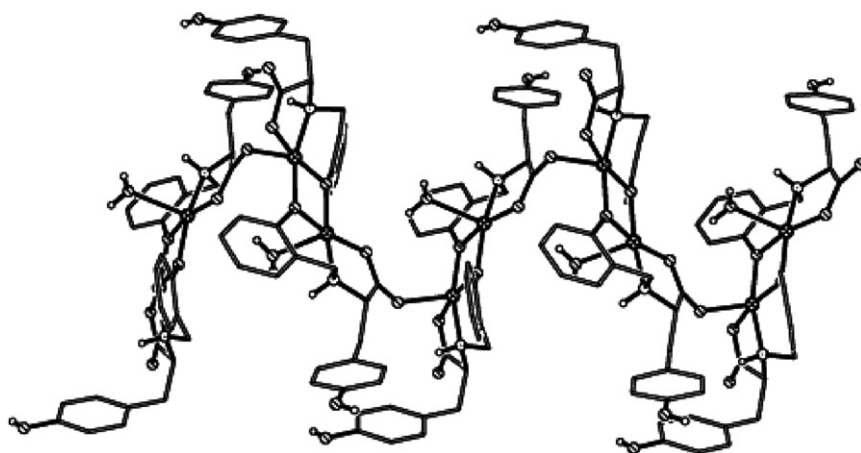
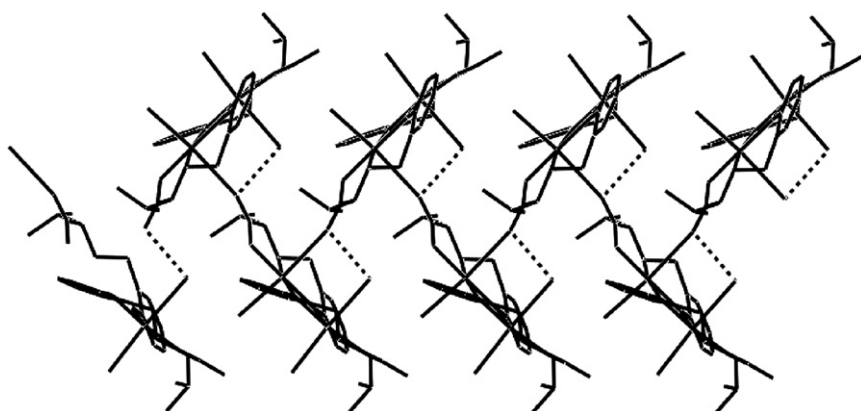


Fig. 3. A portion of the 2D hydrogen-bonded coordination polymer **2**.

Fig. 4. Helical coordination polymer formed by **3**.Fig. 5. A view of a portion of 1D polymer in **5** showing the connectivity.

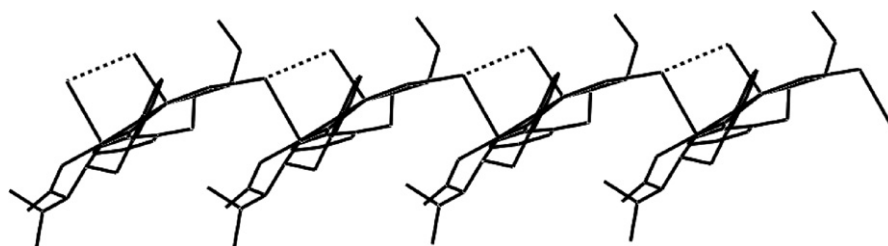
3.1.1. Metal complexes associated with supramolecular isomerism

The phenomenon of supramolecular isomerism can be expected from the conformationally flexible molecules owing to the fact that the energy required to rotate the σ -bonds is comparable to the differences in lattice energy observed between the isomers. The Cu(II) complexes of the ligand H_2Sval have provided such an opportunity to observe supramolecular isomerism. The anhydrous $[Cu_2(Sval)_2]$ obtained by thermal dehydration of $[Cu_2(Sval)_2(H_2O)_3]$, furnished different supramolecular isomers when recrystallized from different solvents.

The connectivity in $[Cu_2(Sval)_2(H_2O)_3]_n$ (**5**) is also very similar to **3** and the repeating dimeric units generate a 1D coordination polymer (Fig. 5). The aqua ligands further participate

in hydrogen bonding with N–H protons and carboxylato oxygen atoms to provide a 2D network structure [6].

Dehydration of **5** followed by recrystallization from water gives a new product, $[Cu_2(Sval)_2(H_2O)] \cdot 2H_2O$ (**6**). Though both have identical molecular formula and the chemical composition, the coordination environment at the metal centre and the formation of the 1D polymer (Fig. 6) are not same and hence the packing is different [6]. With two water molecules in the lattice, **6** has 4 + 1 coordination geometry while **5** adopts 4 + 2 coordination geometry and the differences in the coordination sphere lead to the difference in packing of the 1D polymers. Packing of **6** left no voids for any solvent molecule but **5** provided a cavity of 87 \AA^3 which is about 3% of the unit cell

Fig. 6. A view of a portion of 1D polymer in **6** showing the connectivity.

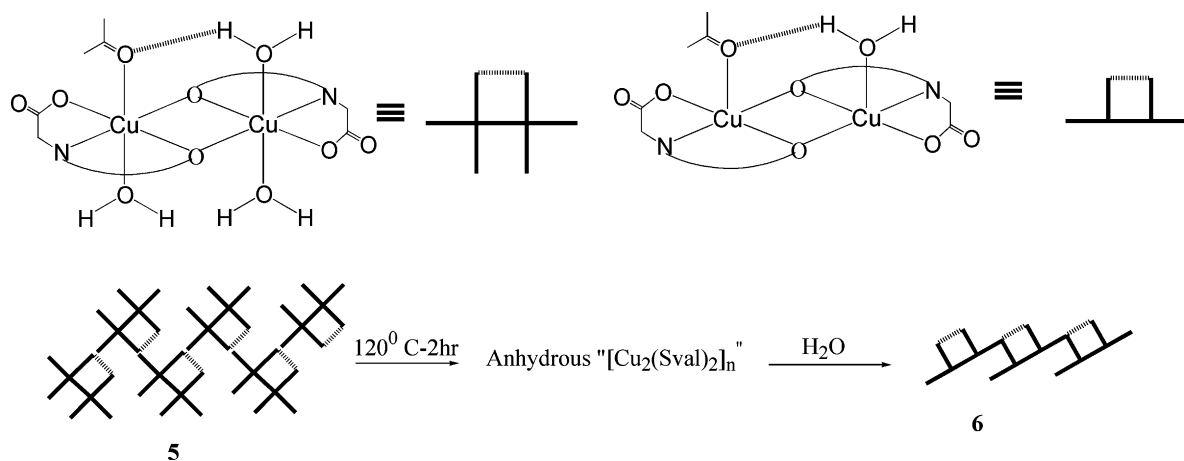


Fig. 7. A schematic diagram showing the formation of two different conformers by simple variation in the first coordination spheres of the building blocks.

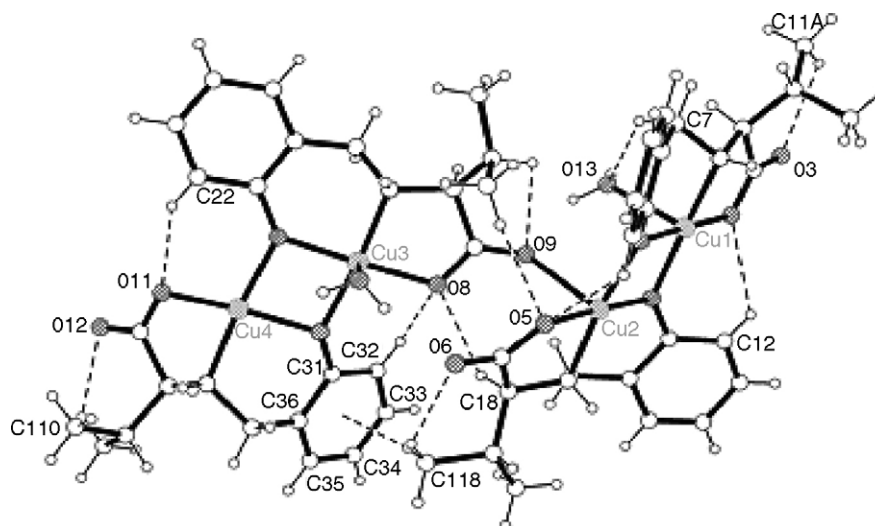
volume. Further, the adjacent dimers are perpendicular to each other in **5** whereas the parallel arrangement of dimers is found in **6**.

The conversion of **5** to **6** is schematically shown in Fig. 7 and these two structures are supramolecular isomers [6].

Recrystallization of anhydrous **5** from 2-propanol gives a 1D polymeric complex $[\text{Cu}_2(\text{Sval})_2(\text{H}_2\text{O})] \cdot 0.5\text{C}_3\text{H}_7\text{OH}$ (**7**) having a structure very similar to **5** [6]. However, the asymmetric unit consists of two crystallographically independent dimers. The coordination geometry around the metal centre is nearly the same as in **5** but conformations and bond distances are slightly different. Unlike **5** and **6**, the two “extra” water molecules are absent in **7** and hence instead of water molecules, the N–H hydrogen atoms are utilized for hydrogen bonding. The 1D polymer chains are arranged parallel to each other and further cross-linked by strong N–H \cdots O–C hydrogen bonds to give a hydrogen-bonded 2D network. The water molecules and the ligand carboxylate O atoms attached to Cu(II) atoms are at the same side of the Cu_2O_2 plane as in **6**, which leads to H–O–H \cdots O hydrogen bonds. The 2-propanol solvent

molecules are partially trapped inside the lattice. The dimeric building blocks **5–7** have several intramolecular C–H \cdots O and C–H \cdots π interactions. Such interactions present in **7** are shown in Fig. 8.

Distinct dimeric units are present in the asymmetric unit of the complex $[\text{Cu}_4(\text{Sval})_4(\text{H}_2\text{O})_2(\text{C}_4\text{H}_9\text{OH})] \cdot \text{C}_4\text{H}_9\text{OH}$ (**8**). The connectivity and conformation are very similar to the earlier example, except that 1-butanol replaces the aqua ligand which occupies the *trans* position. Due to the coordination of Cu(II) to 1-butanol, though the packing of **7** and **8** are similar but the building blocks are different, the repeating unit is not the dimer but tetramer. In addition to the N–H \cdots O interactions observed in **7**, two more H–O–H \cdots O hydrogen bonds are formed between the chains to generate a 2D hydrogen-bonded network [6]. These structural studies revealed that **5** and **6** serve as true examples of structural supramolecular isomers having identical chemical formula but entirely different coordination geometry at the metal centers and hence different packing structures as the coordination spheres of Cu(II) ions are also different due to water molecules.



3.1.2. Solid state supramolecular structural transformations induced by thermal dehydration

In order to rationally design and control the formation of crystal structures, the strategies include the use of various intermolecular forces, from weak van der Waals forces, hydrogen and covalent bonding to ionic interactions. Solid-state supramolecular transformation of one structure into another involves breaking and forming of bonds in more than one direction. It is possible to achieve structural transformations by fine tuning the structure by modifying the components of the ligands employed while controlling the non-covalent interactions [7]. In this connection, the crystal structures discussed in this section exemplify the thermally induced structural transformations associated with dehydration process.

By employing the ligand H_2Sala , a hydrogen-bonded helical coordination polymeric complex $[\text{Cu}_2(\text{Sala})_2(\text{H}_2\text{O})]$ (**9**) was synthesized [8a]. Upon thermal dehydration, the helical coordination polymeric structure of **9** transformed to a 3D coordination network structure in $[\text{Cu}_2(\text{Sala})_2]$ (**10**). The basic dimeric structure of **9** remains intact but the conformation is entirely different in the porous 3D network coordination polymer (Fig. 9) which is obtained by the loss of a water molecule. This structural transformation is irreversible. The conversion of **9** to **10** is the first example of the use of a helical coordination polymer as the building block for a 3D coordination framework with chiral channels and is only the second example where thermal dehydration leads to change in network in the solid state.

The crystal structure of $[\text{Cu}_2(\text{Sgly})_2(\text{H}_2\text{O})]\cdot\text{H}_2\text{O}$ (**11**) first reported by Xu et al. [9], was reinvestigated in our laboratory in detail [8b] and was found to be very similar to **9**. The Cu(II) complex **11** crystallizes as a 1D helical coordination polymer assembled from dimeric building blocks similar to **9**, the major difference being the presence of one more water molecule in the crystal lattice. The complex **10** is obtained from **9** by thermal dehydration at 90°C . Although **9** and **11** have similar packing of helical coordination polymers, a stable anhydrous complex of the later could not be obtained. The anhydrous species rapidly

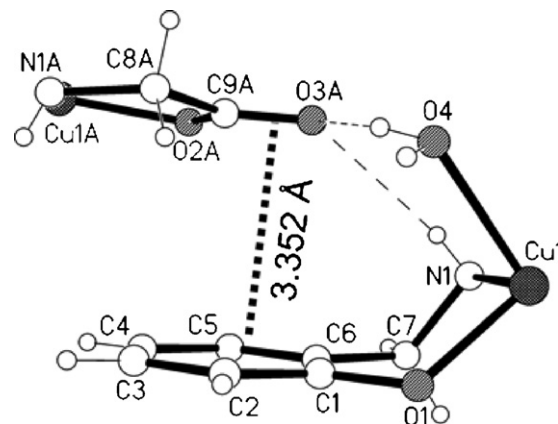


Fig. 10. A view showing the intermolecular $\text{C}=\text{O}\cdots\pi$ interaction in **11**.

gets rehydrated in the presence of air. This reversible hydration, unlike in **9**, can be understood by the close examination of the crystal structure. The carboxylate group and the phenyl ring are almost parallel to each other and are separated by 3.35 \AA in **11** and 3.65 \AA in **9**. This $\text{C}=\text{O}\cdots\pi$ attractive interaction between these two groups, shown in Fig. 10, appears to hold back the carboxylate group to move closer to the aqua ligands and prevents the formation of a new Cu–O bond upon thermal dehydration in the solid-state. The topochemical transformation in **9** can be accounted for by the absence of such an interaction [8b]. This is the first time that a weak interaction such as $\text{C}=\text{O}\cdots\pi$ has been found to have profound influence, not only on the hydrogen-bonding parameters, but also on the thermal dehydration reactions.

$[\text{Zn}_2(\text{Sala})_2(\text{H}_2\text{O})_2]\cdot 2\text{H}_2\text{O}$ (**12**) is another complex having favorable conditions for a topochemical reaction [8c]. Like the Cu(II) complex, coordination of the amine-N generates a new chiral center in the hydrogen-bonded network. Self-assembly of the dimer, sustained by $\text{O}-\text{H}\cdots\text{O}$ and $\text{N}-\text{H}\cdots\text{O}$ hydrogen bonding, leads to the formation of honeycomb-like hydrogen-bonded 3D network structure with the chiral channels all aligned in one direction as shown in Fig. 11.

Anhydrous $[\text{Zn}_2(\text{Sala})_2]$ (**13**) is obtained when all the water molecules are removed by thermal dehydration of **12** and shows a structure very similar to **10** [8c]. The channels are helical and aligned in the same direction. The apical positions occupied by the aqua ligands in **12** are replaced by the carboxylate O in **13**. It appears that formation of new Zn– $\text{O}_{(\text{carboxylate})}$ bond formation is facilitated by both hydrogen-donor N–H groups and hydrogen acceptors in the dinuclear complex. Hence these intermolecular interactions stabilized both the hydrogen-bonded 3D network and 3D coordination polymeric structures. This thermal dehydration is irreversible and **13** cannot be rehydrated, probably due to the formation of a stronger Zn– $\text{O}_{(\text{carboxylate})}$ bond. This is the first example of a topochemical conversion of a hydrogen-bonded supramolecular network to a coordination polymeric structure. Incidentally **13** is isomorphous and isostructural to **10** [10].

It is possible to convert this irreversible structural transformation into a reversible transformation by modifying the components of the ligands. Reversible structural transformations

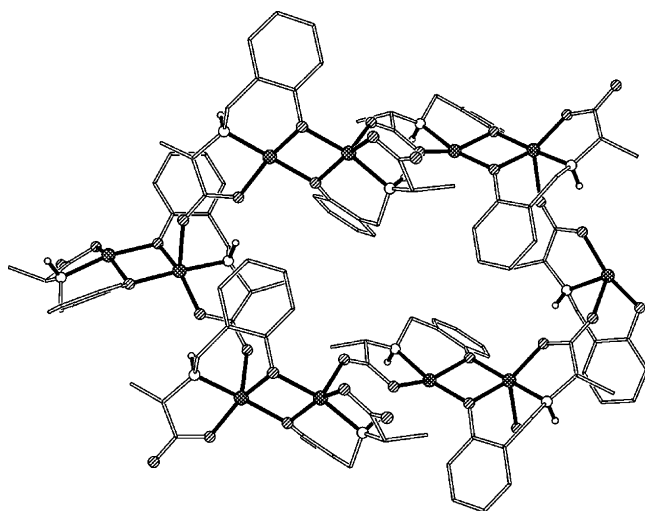


Fig. 9. A portion of the honeycomb-like repeating unit in 3D coordination polymeric **10**.

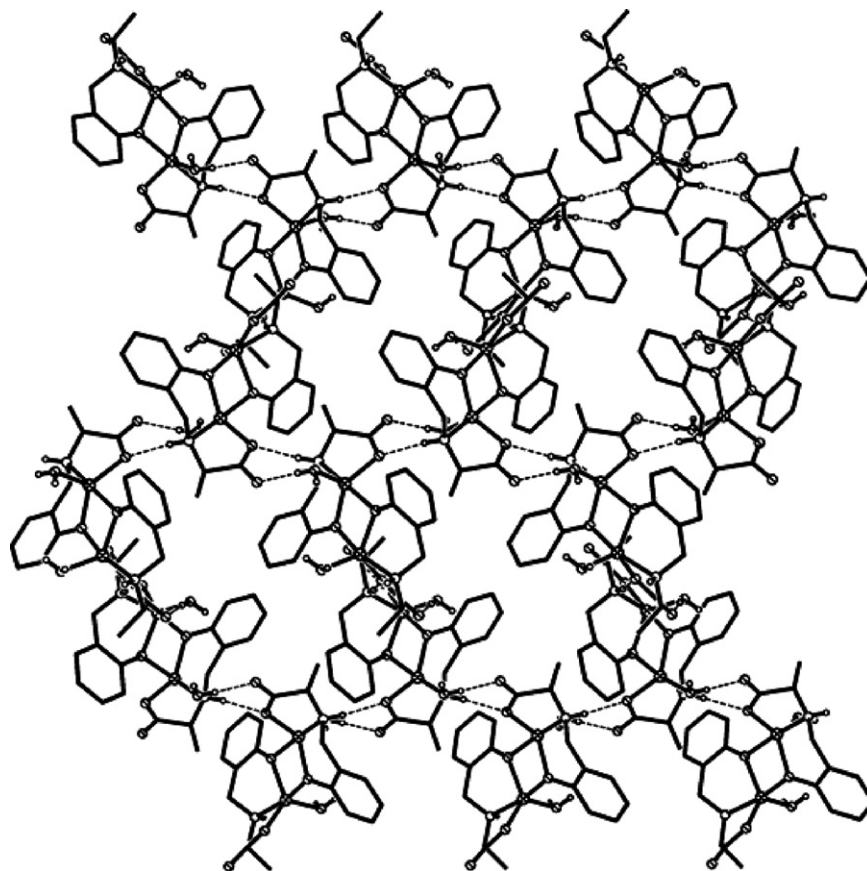


Fig. 11. A view of **12** showing the presence of the chiral channels parallel to the *b*-axis.

are of immense interest for their potential application in molecular switches. For a reversible transformation to be favored, some changes have to be made in the ligands in order to fine tune the structure and to control the non-covalent interactions. In this connection, the 5-substituted H_2MeSala and H_2ClSala ligands are employed for complexation with $\text{Zn}(\text{II})$ in the presence of LiOH to obtain $[\text{Zn}_2(\text{ClSala})_2(\text{H}_2\text{O})_2] \cdot 2\text{H}_2\text{O}$ (**14**) and $[\text{Zn}_2(\text{MeSala})_2(\text{H}_2\text{O})_2] \cdot 2\text{H}_2\text{O}$ (**15**) [10]. With the exception of the -methyl and -chloro substituents, both **14** and **15** are isomorphous and isostructural with **12**. In these hydrogen-bonded network structures, a honeycomb-like chiral cavity is

formed by six dinuclear units. The differential thermogravimetric (DTG) patterns of **14** and **15** are entirely different from **12**. While **12** is completely dehydrated below 110°C , the dehydration is only up to 90% in **14** and **15**. The remaining water is lost at $\sim 180^\circ\text{C}$ in **14** and at $\sim 220^\circ\text{C}$ in **15**. This change in DTG behavior can be explained by the fact that the bulky para-substituents occupy the channels in the lattice thus hindering passage of water during thermal dehydration. However, the resulting anhydrous compounds can be regenerated as hydrated compounds, **14** and **15** upon recrystallization from water or aqueous MeOH as shown in Fig. 12. The reason for

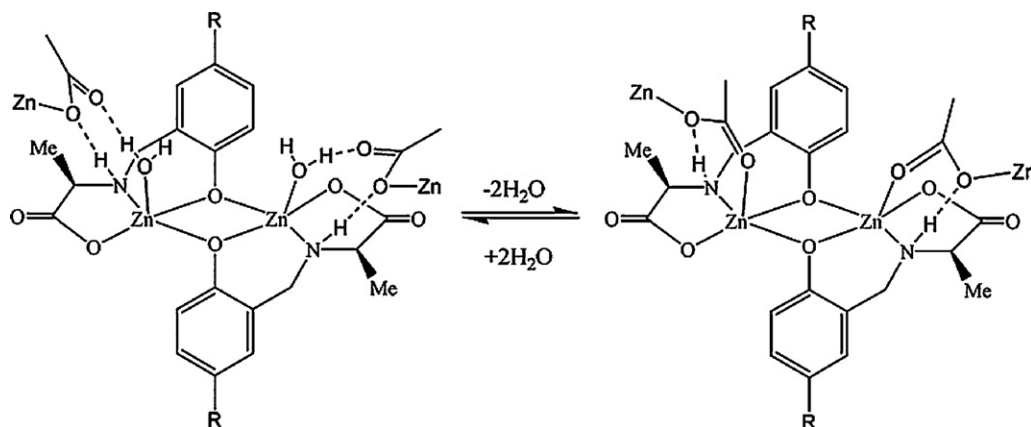


Fig. 12. A scheme illustrating the reversible structural transformation from hydrogen-bonded network to covalent bonded network by thermal dehydration.

the dehydrated compounds to become hydrated during crystallization from aqueous solution has been attributed to the repulsive interactions between the substituents and atoms in the other parts of the 3D coordination network and the inter-conversion of structures is driven to alleviate these repulsive interactions.

3.1.3. 3D coordination polymer with star-like cavity

It may be noted that the connectivity observed in 3D structures of **10**, **12**–**14** has diamondoid architecture. For a given ligand with flexible conformation, the conversion of one structure to another may be possible by altering the conditions such as pH, counter ions, solvent, temperature, concentration, time, etc. In this section the role of the nature of solvents on the crystallization of $[\text{Cu}_2(\text{Scp11})_2(\text{H}_2\text{O})_2]$ containing a non-chiral $\text{H}_2\text{Scp11}$ ligand has been discussed, while highlighting the single pot crystallization furnishing coordination and hydrogen-bonded polymeric structures, and the star-like channels observed in $[\text{Cu}_2(\text{Scp11})_2]$.

Recrystallization of $[\text{Cu}_2(\text{Scp11})_2(\text{H}_2\text{O})_2]$ (**16**) obtained from the reaction of $\text{H}_2\text{Scp11}$ with $\text{Cu}(\text{OAc})_2$ in equimolar ratio, from DMF/acetone solvent, furnishes rod-like bluish-green crystals of $[\text{Cu}_2(\text{Scp11})_2(\text{H}_2\text{O})_2] \cdot 2\text{Me}_2\text{CO}$ (**17**), along with green cubic crystals of $[\text{Cu}_2(\text{Scp11})_2] \cdot \text{H}_2\text{O}$ (**18**) [11]. The dimeric building block, $[\text{Cu}_2(\text{Scp11})_2]$ in **18** assembles to form a 3D coordination polymeric network structure in the space group $Ia\bar{3}d$ (No. 230). The topology of connectivity can be described in terms of a hexagonal diamondoid architecture. The star-like channel, as shown in Fig. 13, is created by the packing of molecules and has about 27% empty space in the crystal lattice which is partially occupied by water molecules. When the DMF

solution is evaporated **16** is regenerated. Anhydrous **18** absorbs moisture and this species shows identical thermal behavior to that of **16** which may indicate that **16** and **18** have different crystal structures and, perhaps the removal of aqua ligands can be reversible as found in the previous examples. The hexagonal diamondoid 3D network topology observed in **18**, compared to cubic diamondoid 3D network structures discussed in the previous sections, shows that it is often possible to generate different yet closely related structures by replacing the substituents on the amino acid side arm and by inducing conformational changes on the flexible backbone of the reduced Schiff base ligands.

3.1.4. Hydrogen-bonded 1D coordination polymers forming supramolecular networks

In this section, a series of dicopper(II) complexes of reduced Schiff base ligands derived from $-\text{Cl}$, $-\text{Me}$, or $-\text{OH}$ substituted salicylaldehydes and aminocyclopentane/cyclohexanecarboxylic acids and *L*-alanine are discussed. All these complexes contain phenolato bridged dinuclear Cu_2O_2 cores with $\text{Cu} \cdots \text{Cu}$ distance of *ca* 3 Å. The crystal packing of dimers resulted in the formation of various hydrogen-bonded polymeric structures and the different crystal structures described here exemplify the role of solvents and aqua ligands in the formation of intermolecular hydrogen bonds in generating interesting supramolecular networks.

Recrystallization of **16** from methanol gives $[\text{Cu}_2(\text{Scp11})_2(\text{MeOH})_2]$ (**19**) where the apical positions are occupied by the methanol group in a *trans* fashion [12]. A 1D polymeric structure in **19** is generated by $\text{MeOH} \cdots \text{O}=\text{C}$ and $\text{N}-\text{H} \cdots \text{O}=\text{C}$ intermolecular hydrogen bonding. $[\text{Cu}_2(\text{ClScp11})_2(\text{DMF})(\text{H}_2\text{O})] \cdot \text{MeCN}$ (**20**), $[\text{Cu}_2(\text{MeScp11})_2(\text{MeOH})_2] \cdot 2\text{MeOH}$ (**21**), $[\text{Cu}_2(\text{ClSch11})_2(\text{MeOH})_2] \cdot 2\text{MeOH}$ (**22**) and $[\text{Cu}_2(\text{OHScp11})_2(\text{H}_2\text{O})_2]$ (**23**) are obtained from the respective $\text{H}_2\text{ClScp11}$, $\text{H}_2\text{MeScp11}$, $\text{H}_2\text{ClSch11}$ (*N*-(2-hydroxy-5-chlorobenzyl)-1-aminocyclohexanecarboxylic acid) and $\text{H}_2(\text{OH})\text{Scp11}$ ligands [12]. Complexes **19**–**23** display Cu(II) centers with distorted square pyramidal geometry. The common 1-aminocyclopentanecarboxylate side arm of the ligands in **19**–**23** results in the formation of five-membered chelate rings. In general, the apical sites of the dimeric Cu(II) centers with square-pyramidal geometry are occupied by the solvent molecules in an *anti* fashion. Packing of the dimeric units in **19**–**22** results in a 1D hydrogen-bonded polymeric structures supported by intermolecular hydrogen bonds generated among amine H atoms, solvent molecules and carboxylate oxygen atoms as well as weak interactions of the neighboring carboxylate oxygen atoms with each Cu(II) ion; **21** and **22** are isomorphous but not isostructural. However, packing in **23** is different resulting in the formation of a 3D hydrogen-bonded network due to the additional intermolecular hydrogen bonds arising from the hydroxy group on the phenyl ring with the aqua ligands and carboxylate oxygen atoms, besides the hydrogen bonding from $\text{N}-\text{H}$ hydrogen and carboxylate oxygen. Hence the crystal packing and dimensionality of the supramolecular network, sustained by non-covalent interactions such as hydrogen bonds, can be controlled by fine tuning the ligand structure in terms of hydrogen bond donors and acceptors.

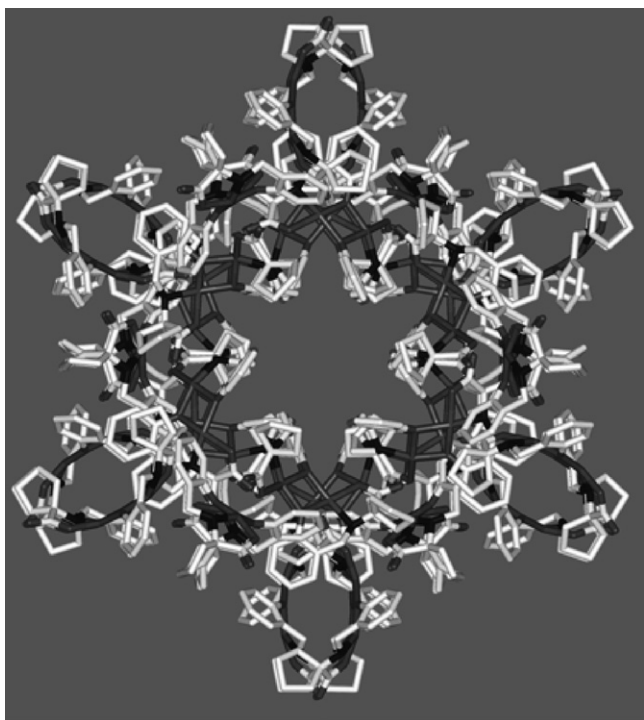


Fig. 13. Star-like cavity in **18** viewed from threefold rotation axis.

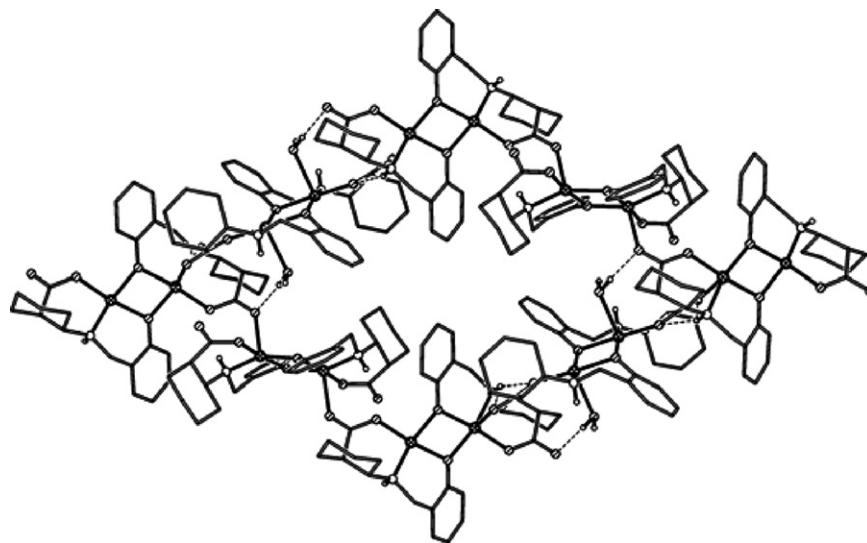


Fig. 14. A portion of the square-grid network connectivity in **24**.

$[\{Cu_2(Sch12)_2\}_2Cu_2(Sch12)_2(H_2O)_2] \cdot 4H_2O$ (**24**) has three independent dinuclear units [12] in the asymmetric unit. One of the Cu(II) centers has an aqua ligand in the apical position and the oxygen atom of the carboxylato group from this unit is bound to another Cu(II) center. The lattice water and the carbonyl oxygen participates in hydrogen bonding to produce a 2D coordination polymeric structure and the inter-dimer connectivity leads to the formation of a square-grid network structure as shown in Fig. 14. Presence of strong inter-dimer antiferromagnetic coupling is suggested by the variable-temperature magnetic studies [12].

Square-planar geometry at the Cu(II) center is displayed by $[Cu_2(ClSch12)_2] \cdot 2MeOH$ (**25**). Both the methanol molecules are involved in hydrogen bonding with the amine nitrogen and carboxylate oxygen atom to form a 1D polymeric structure [12] as displayed in Fig. 15.

Recrystallization of $[Cu_2(Diala)_2(H_2O)_2] \cdot H_2O$ from DMSO/acetone gives the dark-green dimer, $[Cu_2(Diala)_2(DMSO)_2] \cdot 2DMSO \cdot 2Me_2CO$ (**26**). In the solid-state structure, two of the four DMSO molecules are bonded to the Cu(II) in the dimer and the remaining two are hydrogen bonded to the amine hydrogen atoms. The bulkiness of the DMSO molecules causes them

to be disposed in *anti* fashion. This in turn results in the formation of a pseudo-center of inversion which is very unusual for the complexes having chiral reduced Schiff-base ligands [12]. Acetone molecules fill the empty cavities between the parallel strands formed by the complementary hydrogen bond between the phenolic hydrogen and oxygen atoms of the carboxylate group.

In $[Cd(HSasp)(H_2O)_2]_n$ (**27**) the seven coordinated Cd-center is surrounded by tetradentate HSasp which bonds through phenolate O, secondary amine N, one α -carboxylic O and one β -carboxylic O [13]. The coordination geometry is completed by two water molecules and bridging β -carboxylic oxygen from the neighboring unit to form a 1D zigzag chain. The α -carboxylic group from the adjacent unit forms a hydrogen bond with the N–H proton to give a 2D-layered structure.

3.1.5. Schiff base versus reduced Schiff base ligands: A case study

Apart from the reduced Schiff base ligands with carboxylate donor group, their sulfonic acid analogues are expected not only to improve the solubility in aqueous media but also form interesting supramolecular architectures by modifying the con-

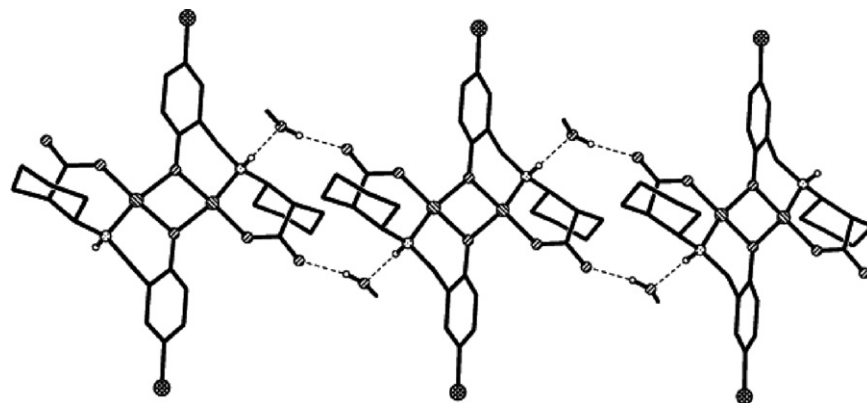


Fig. 15. A view of the 1D hydrogen-bonding network in the crystal structure of **25**. Hydrogen atoms are omitted except those involved in hydrogen bond formation.

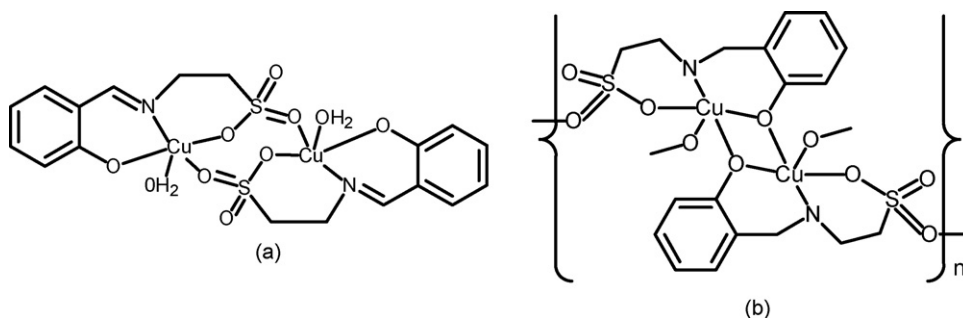


Fig. 16. Schematic diagrams showing the connectivity in (a) **28** and (b) **29**.

nectivity at the metal centers as well as the hydrogen bonding pattern. In this context, dinuclear copper(II) complexes of *N*-(2-hydroxybenzyl)-aminomethane/ethanesulfonic acids in the form of both Schiff base and reduced Schiff base ligands have been employed. A striking difference observed is that the Schiff bases H_2Sams and H_2Saes furnished eight membered dicopper(II) centers with the sulfonate group as bridging moiety whereas the reduced Schiff bases H_2Sam and H_2Sae formed the phenoxo bridged Cu_2O_2 cores. Herein, different structural features between Schiff base and reduced Schiff base dicopper(II) complexes have been highlighted.

The change in complexation behavior that may occur by the reduction of $C=N$ bond in Schiff base species is illustrated by the two $Cu(II)$ complexes, $[Cu_2(Saes)_2(H_2O)_2] \cdot 2H_2O$ (**28**) and $[Cu_2(Sae)_2] \cdot 2H_2O$ (**29**) containing the Schiff base, $Saes^{2-}$ and the corresponding reduced Schiff base, respectively [14]. The copper centers in **28** each assume a square pyramidal geometry with the apical positions occupied by a sulfonate oxygen atoms thus forming a eight-membered sulfonato-bridged dinuclear complex (as shown in Fig. 16a); in addition to this, the $Saes$ dianion forms two six-membered rings. The dimers are packed in the solid state to give a hydrogen-bonded 2D structure. Two types of complementary hydrogen bonds are present: the first one is between the phenoxo oxygen and one of the hydrogen atoms of the aqua ligand from the adjacent dimer; the next one is between the free oxygen atoms of the sulfonate group with another hydrogen atom of the aqua ligand. In addition, the resulting 2D sheets are also supported by $C-H \cdots O$ hydrogen-bonding interactions.

In **29**, the Sae ligand with flexible backbone behaves like other reduced Schiff-base ligands in terms of forming a phenolato-bridged $Cu(II)$ dimer with Cu_2O_2 core (as shown in Fig. 16b). The apical site on each $Cu(II)$ center is occupied by an oxygen atom of the sulfonate group from the neighboring dimer. This inter-dimer connectivity leads to the formation of a square-grid network structure. The two axial oxygen atoms have trans geometry due to the crystallographic center of inversion present at the center of the Cu_2O_2 ring. Interestingly the infinite 2D network structure with (4,4) net formed in **29** is the first of its kind observed in the $Cu(II)$ and $Zn(II)$ complexes containing reduced Schiff-base ligands although these nets are ubiquitous in the literature [15]. Recrystallization of **29** from strongly coordinating DMF leads to the formation of $[Cu_2(Sae)_2(DMF)_2] \cdot 2DMF$ (**30**). The axial sulfonate groups in **29** are replaced by DMF

molecules in **30** and hence a discrete dinuclear compound is formed. Two more DMF molecules were found in the crystal lattice. The crystal packing of **30** generates 2D hydrogen-bonded polymeric structures with $N-H \cdots O$ hydrogen bonding between one of the sulfonate oxygen and NH hydrogen atoms (Fig. 17).

$[Fe_2(\mu-OH)(\mu-OAc)(S-Simd)_2] \cdot 4H_2O$ (**31**) and $[Fe_2(\mu-OH)(\mu-OAc)(R-Simd)_2] \cdot 2H_2O$ (**32**) are obtained by the reaction of $Fe(NO_3)_3 \cdot 9H_2O$ in the presence of $NaOAc$ with $S-H_2Simd$ and $R-H_2Simd$, respectively [16]. Both crystals are similar, but due to the presence of an opposite chiral center in the ligand, **31** contains right-handed 1D helical channels with a diameter of 7.3–9.8 Å whereas **32** has a left-handed helical channels as shown in Fig. 18. In the crystal structure of **31**, the hexagonal channels are filled with water. The crystals of **32** have identical but left-handed helices. This situation is very similar to that found by our group for $[Cu_2(D-Sala)_2(H_2O)]$ and $[Cu_2(L-Sala)_2(H_2O)]$ [5]. A notable feature of the molecule is the formation of a crescent moon shaped hydrophilic binding site formed by lining up the hydroxo bridge (H-bond donor) and all four oxygen atoms of the carboxylate oxygen (H-bond

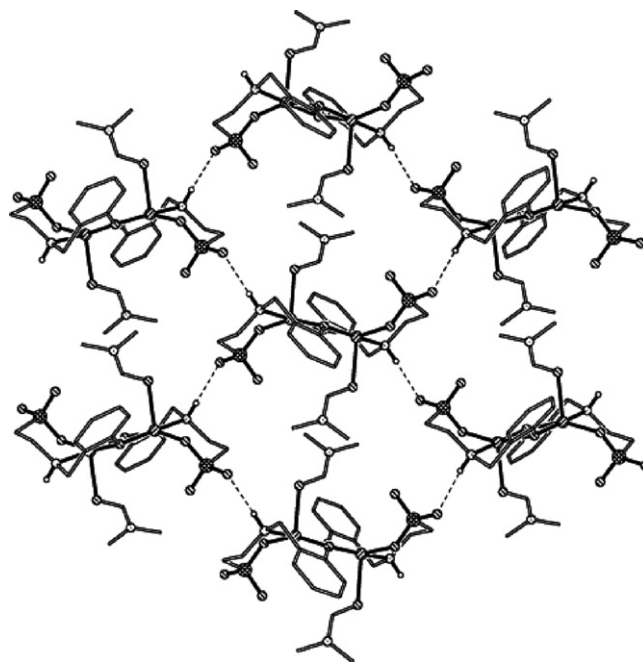


Fig. 17. Hydrogen bond connectivity in **30**.

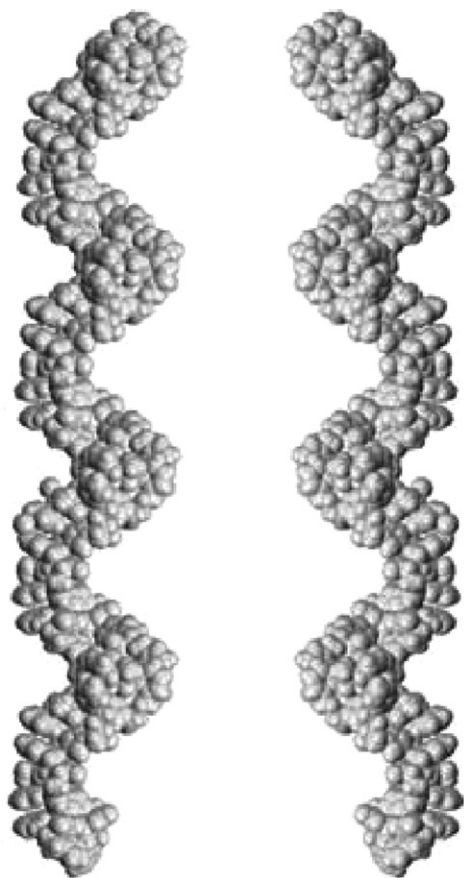


Fig. 18. Left and right handed helices of **31** and **32**.

acceptor). The helical channels are formed by docking of dimers on top of each other rotated by 60° and connected through intermolecular hydrogen bonding between imidazole proton and phenolate oxygen. The helical array of acidic protons together with a hydrophilic cavity inside the channel has the potential to influence binding and reaction inside the channel. Two differ-

ent types of H-bonded waters are present: (a) water inside the channel and (b) one forming a bridge between two neighboring **31** species. As the waters inside the channel are loosely bound compared to the other water, the former can be removed easily as shown by the loss of water over two different temperature ranges (<100 and $100\text{--}140^\circ\text{C}$) in **31** and **32**; the channels can be refilled.

3.1.6. Helical staircase coordination polymer hosting helical water chain

Besides the ligands with an amino acid side arm having simple carboxylate donor, the ligands with additional active donor groups such as --COO^- in the side chain have displayed interesting intermolecular connectivity, as expected, while generating several 1D coordination polymeric structures in Cu(II) and Ni(II) complexes. Interestingly, a Ni(II) complex, $[(\text{H}_2\text{O})_2 \subset \{\text{Ni}(\text{HSglu})(\text{H}_2\text{O})_2\}] \cdot \text{H}_2\text{O}$ (**33**) derived from *N*-(2-hydroxybenzyl)-*L*-glutamic acid (H_3Sglu) displays a novel helical staircase coordination polymeric structure encapsulating 1D helical water chain in the chiral helical channels [17]. Of the two carboxylate groups in the HSglu^{2-} ligand, one is chelating intramolecularly, while the second carboxylate ion coordinates to a neighboring Ni(II) atom to furnish staircase coordination polymers. Although helical coordination polymers are ubiquitous staircase polymers with channels are rare in coordination polymer structures [18]. The octahedral coordination at the Ni(II) centre is completed by two aqua ligands. Of the six lattice water molecules present in the asymmetric unit, two of the four inside the helical pore are hydrogen bonded to produce a 1D helical polymer as shown in Fig. 19. Hydrogen bonding is propagated by the other two water molecules *via* helical water chain and aqua ligands. The two water molecules outside the helical pore occupy empty space in the lattice.

Dehydration leads to the collapse of the single crystalline nature as the free standing staircase polymers are not supported by strong non-covalent interactions. It is well known that a chi-

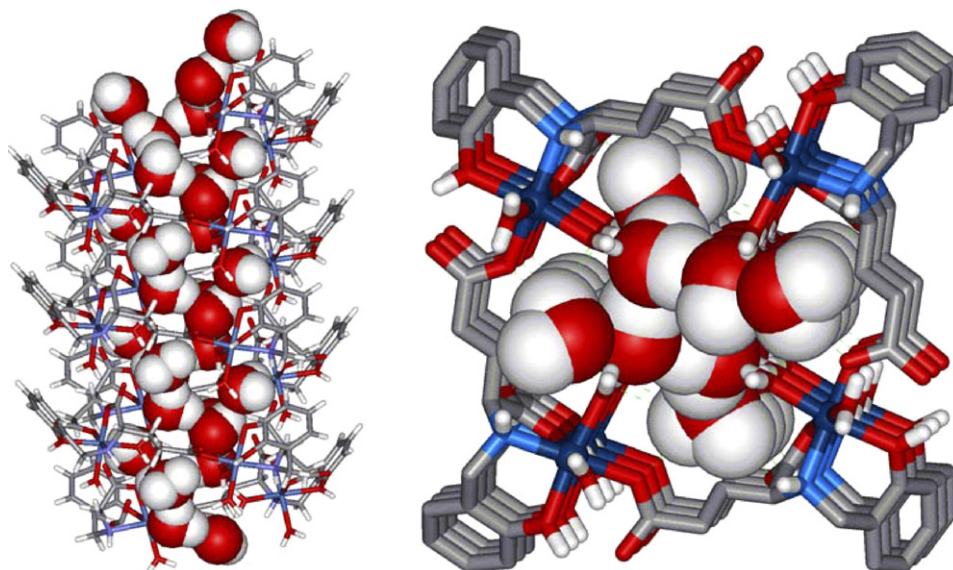


Fig. 19. Side and top views of 'helix inside a helix' are shown. The helical hydrogen-bonded chain of water molecules fill the space inside the helical staircase coordination polymer **33**.

ral ligand can often lead to the formation of helical structure [18]. The presence of one or more non-chelating side arms in a chiral ligand may provide the possibility for selective and complementary aggregation of the metal complexes. Among various metal complexes investigated, only the Ni(II) complex of the chiral ligand H₃Sglu, has been found to generate helical staircase coordination polymer. The structure of the left-handed helical coordination polymer, **33** encapsulating the hydrogen-bonded helical stream of water molecules inside its helical cavity illustrates a novel cooperative assembly and recognition of water molecules in the inorganic crystal host. These results may exemplify the maxim that the structural constraints operating on orientation of water by its surroundings and *vice versa* can be very significant.

In contrast to **33**, Cu(II) shows a square pyramidal geometry and connectivity of the neighboring carboxylate oxygen atoms with Cu(II) centers results in a 1D zigzag coordination polymer in the crystal structure of [Cu(HSglu)(H₂O)]·H₂O (**34**) [17]. The fifth position is occupied by the aqua ligand. The structures of **33** and **34** derived from the same H₃Sglu ligand serve as good examples to demonstrate that the overall topology of the system depends not only on the nature of the metal but also on the coordination geometry around it.

3.1.7. Influence of cation on molecular assembly

Reaction of H₂^tBuGly with Na₂MoO₄·2H₂O in aqueous methanol gives [Na₄(H₂O)₄(μ-H₂O)₂]·[Mo₂O₅(^tBuGly)₂]₂ (**35**) while in the presence of excess CsCl [Cs₂{Mo₂O₅(^tBuGly)₂}]·H₂O (**36**) is produced [19]. In **35** a rectangular Na₄⁴⁺ cluster is formed which further binds to six O atoms to form a Na₄O₆ cluster like a dicubane with two extreme and opposite corners removed. The oxygen atoms of *cis*-MoO₂ form hydrogen bonds with N–H protons to generate hydrogen-bonded 1D chains. The chains further interact to form a hydrogen-bonded 2D network. In **36**, Cs⁺ forms a 1D-helical chain stabilized by carboxylate oxygen and Mo–O. In **35**, water is able to bridge two Na⁺ ions whereas this is not observed in **36**. For the same reason, an oxygen of the carboxylate group of the ligand can bind to three Na⁺ ions in **35**, while it binds to two Cs⁺ in **36**.

3.2. Type 2: Metal aggregates and oligomeric building blocks

The asymmetric compartmental ligand, H₂Pipala, reacts with Cu(OAc)₂·H₂O to give the tetranuclear complex, [Cu₄(Pipala)₂(CH₃COO)₄]·2CH₃CN·2H₂O (**37**). The structure consists of two dinuclear units, in each unit the ligand acts as pentadentate donor and bridges the Cu(II) ions. The Cu(II) centers are further bridged by two acetate groups in a *syn-syn* manner within the unit. The two dimeric units are bridged by the carboxylate oxygen to form a centrosymmetric four-membered ring (Fig. 20). Due to the constraints imposed by the piperazine ring, which is present in a boat form, the Cu(II) ions deviate from ideal square pyramidal geometry to distorted octahedral geometry [20].

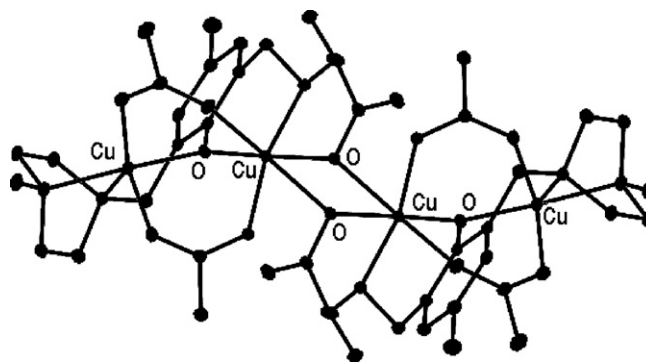


Fig. 20. The structure of **37** showing the dinuclear units connected by the bridging carboxylate oxygen. Hydrogen atoms and solvent molecules are omitted.

Exemplifying that the reduced Schiff base ligands have the potential for generating fascinating supramolecular network structures, Ray et al. have reported an octameric Cu(II) complex [Cu₈(Simd)₈Py₁₀]·Py·3MeOH·(C₂H₅)₂O (**38**; Py = Pyridine), with a novel capsule-like cavity capable of hosting pyridine molecules by employing a tetradentate H₂Simd ligand [21]. The trapped pyridine molecules were held inside the cavity *via* an interesting combination of hydrogen and coordination bonds as described in the following section.

The octameric Cu(II) complex, **38** consists of two slightly different cup-shaped tetrameric units [21]. The two cup-like units form a capsule that is held together by eight hydrogen-bonding interactions between the imidazole NH groups of one tetramer and non-bonded carboxylate-oxygen atoms of the other tetrameric unit. In both the tetrameric units, one side of the square is effectively closed by the arrangement of the four-phenolate rings from the ligands. Two pyridine molecules are trapped side by side in the cup-shaped bottom unit by hydrogen

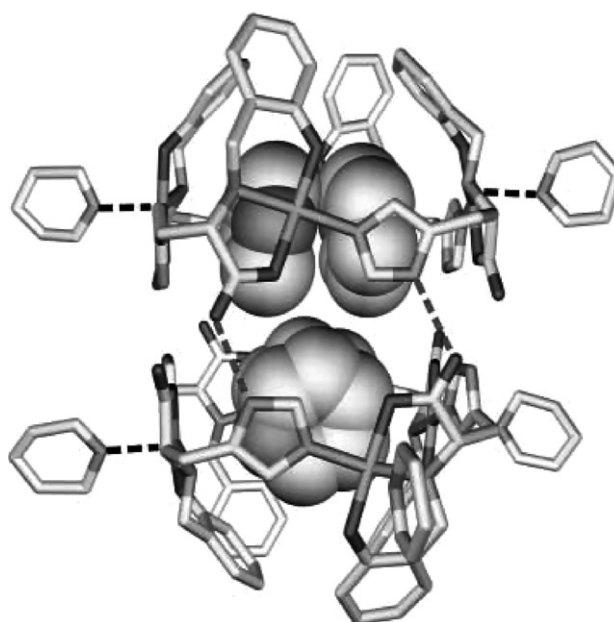


Fig. 21. Molecular structure of **38**. Solvent molecules are omitted for clarity. Adapted from Ref. [21] and reproduced with permission.

bonding to the amine N atom of the ligand as shown in Fig. 21. Four pyridine molecules bind to four Cu(II) externally. Interestingly, in the top half of the capsule unit, the trapped pyridines are bonded to two of the Cu(II) centers (instead of being involved in hydrogen bonding as in the bottom half of the capsule). In the bottom half of the capsule each Cu(II) ions is bonded to a pyridine externally but the top half two Cu(II) ions are bonded to the pyridine molecules externally and the other two internally. Thus the two halves exhibit contrasting binding with the guest molecule. Such molecular cavities offer potential applications as selective hosts for anion sensing, catalysis, selective recognition and separation.

4. Metallasupramolecular structures derived from *N*-(2-pyridyl)-amino acid ligands

The NNO coordination mode is quite common in biological systems. The pyridine ring influences the basicity of the amine group and the electronic structure of the ligand is different from the 2-hydroxybenzyl ligand. One hidden coordination site is the carbonyl oxygen, which may participate in weak hydrogen bonding or may coordinate with metal centers from the neighboring molecule to give rise to interesting connectivity and hence network structure. The amine hydrogen and the oxygen in the

ligands are expected to form hydrogen bonds with the neighboring molecules. The chiral center of the amino acid and the diversity of the substituent groups from the amino acid side arm are other factors that play a part in the assembly of fascinating supramolecular structures.

4.1. Influence of cation and pH on metallacrown cations

Metallacrowns (MCs) with a variety of structural types can also be obtained by the self-assembly of metal ions and the reduced Schiff base ligands. In general, MCs are robust in solution and this property can be employed for exchange reactions with metal ions and anions. The selectivity is determined not only by the cavity size of the MC but also by the radii of the ions used. This “host–guest” chemistry of Cu(II) compounds containing reduced Schiff base ligands that gives structurally different MC cations in the presence and absence of Li^+ in the cavity is illustrated here. The MC cations are very labile in our system with Cu(II) ions and the pH of the solution also found to play an important role.

Hphis reacts with $\text{Cu}(\text{ClO}_4)_2 \cdot 6\text{H}_2\text{O}$ to form a 1D coordination polymeric species, $[\text{Cu}(\text{Hphis})(\text{H}_2\text{O})](\text{ClO}_4)_2$ (**39**) [22]. In the cation, the Cu(II) center is five-coordinate, with the tridentate phis ligand bonded in a *mer* fashion at the square base

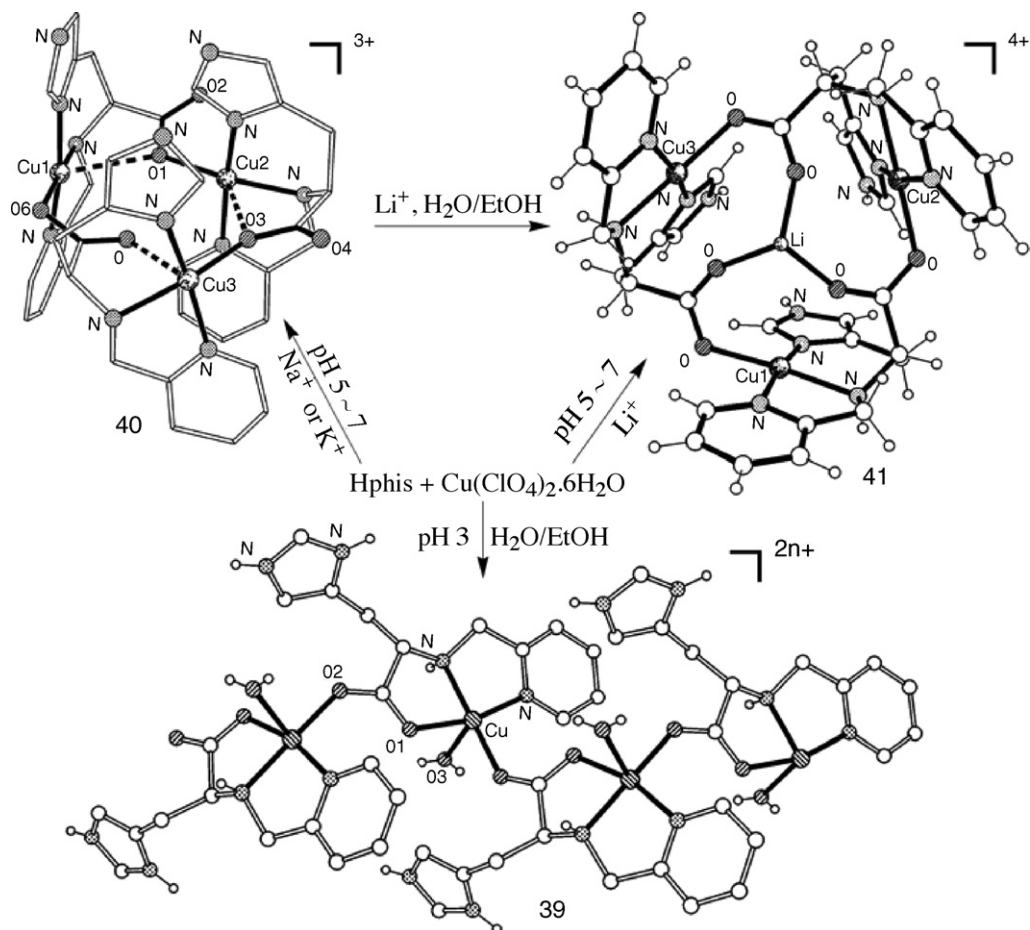


Fig. 22. pH dependent interconversion of **39–41**.

and the fourth position completed by a carboxylate oxygen from the neighboring repeating unit. A water molecule at the apex completes the distorted square pyramidal geometry at the Cu(II) center. The second carboxylate oxygen atom participates in intermolecular bonding to Cu(II) which generates a 1D zigzag polymeric structure.

When the potassium salt of phis reacted with $\text{Cu}(\text{ClO}_4)_2 \cdot 6\text{H}_2\text{O}$ in a 1:1 molar ratio, dark blue crystals of $[\text{Cu}_3(\text{phis})_3](\text{ClO}_4)_3 \cdot 2\text{H}_2\text{O}$ (**40**) were isolated [22]. In the structure of the trinuclear cation as shown in Fig. 22, each Cu(II) is surrounded by a phis ligand in a *mer* fashion, and the donor atoms occupy the base of the square pyramid along with another carboxylate oxygen from the neighboring cation. The apical position of the distorted square pyramid is occupied by the oxygen atoms of the carboxylate group of the neighboring phis ligand. The oxygen atoms O(1) and O(3) are bridging Cu(II) atoms while O(2) and O(4) atoms are non-bonded. This makes the cavity in the ring very small, and the shortest distance, 3.03 Å, is between O(1) and O(5). This [8-MC-3] metallacrown cation is very unsymmetrical with Cu...Cu distances, 3.86, 4.31, and 5.27 Å. Such copper compounds have been used as a structural model for the trinuclear site in ascorbate oxidase from green zucchini [23].

The compound $[(\text{ClO}_4)\text{Li} \subset \text{Cu}_3(\text{phis})_3](\text{ClO}_4)_3 \cdot 3\text{H}_2\text{O}$ (**41**) has been isolated when a molar equivalent of LiClO_4 was added to **40** [22]. The same compound could also be obtained from the lithium salt of phis and $\text{Cu}(\text{ClO}_4)_2 \cdot 6\text{H}_2\text{O}$ in a 1:1 molar ratio. The crystal structure shows that the asymmetric unit consists of the $[(\text{ClO}_4)\text{Li} \subset \text{Cu}_3(\text{phis})_3]^{3+}$ cation, three strongly hydrogen-bonded lattice water molecules, and three perchlorate anions interacting with the cations and lattice waters. The trinuclear cation has the shape of a cone in which the phenyl rings are on the same side as observed in **40**. The N–H protons of the imidazole groups at the bottom are hydrogen bonded to oxygen atoms of the three water molecules. The $[\text{Li} \subset \text{Cu}_3(\text{phis})_3]^{4+}$ cation has an idealized C_3 symmetry with three crystallographically

independent Cu(II) centers. It is obvious that the $[\text{Cu}_3(\text{phis})_3]^{3+}$ cation, [8-MC-3], has structurally reorganized to accommodate a LiClO_4 . The pH dependent interconversion of **39–41** is summarized in Fig. 22.

4.2. Influence of the nature of reactants on metallacrown cations

In addition to the nature of the cations used and the pH of the solution, the stoichiometry of the reactants also plays a vital part in the formation of metallacrown cations. In this connection, the reactivity of $[\text{Cu}(\text{pgly})_2] \cdot 2\text{H}_2\text{O}$ (**42**) under different conditions is discussed here.

The reaction between $\text{Hpgly} \cdot \text{HCl}$ and $\text{Cu}(\text{ClO}_4)_2 \cdot 6\text{H}_2\text{O}$ or $\text{Cu}(\text{CH}_3\text{COO})_2 \cdot \text{H}_2\text{O}$ in the molar ratio of 2:1 furnished dark blue crystals of $[\text{Cu}(\text{pgly})_2] \cdot 2\text{H}_2\text{O}$ (**42**). Complex **42** has two tridentate pgly ligands, each bonded to Cu(II) in a *facial* manner [24]. The molecule has a crystallographic inversion center at Cu(II) in which the Cu(II) has distorted octahedral geometry with a *trans*- N_4O_2 donor set. The N–H donor and C=O acceptor groups in the pgly ligand and water in the lattice participate in the hydrogen bonding and form an interesting 2D sheet structure in the *bc* plane in which the hydrogen atoms from water molecules bound to two different oxygen atoms and fill the empty space in the lattice. The hydrogen bonds are considered to be of medium strength because the D...A distances vary from 2.81 to 2.99 Å. Mononuclear $\text{Zn}(\text{pgly})_2 \cdot 2\text{H}_2\text{O}$ (**43**) has a very similar structure to that of the Cu(II) complex [25].

When **42** was reacted with an equivalent amount of $\text{Cu}(\text{ClO}_4)_2 \cdot 6\text{H}_2\text{O}$ in H_2O – MeOH solution, dark blue hexagonal crystals of $[\text{Cu}_6(\text{pgly})_3(\text{spgly})_3](\text{ClO}_4)_6 \cdot 9\text{H}_2\text{O}$ (**44**) were isolated. X-ray crystallographic analysis shows that the hexameric cation consists of two crystallographically independent Cu(II) atoms, a reduced Schiff base ligand (pgly) and, surprisingly, a Schiff base ligand (spgly) in the asymmetric unit [24] as shown in Fig. 23. Each tridentate ligand is bonded to Cu(II) in a *meridi-*

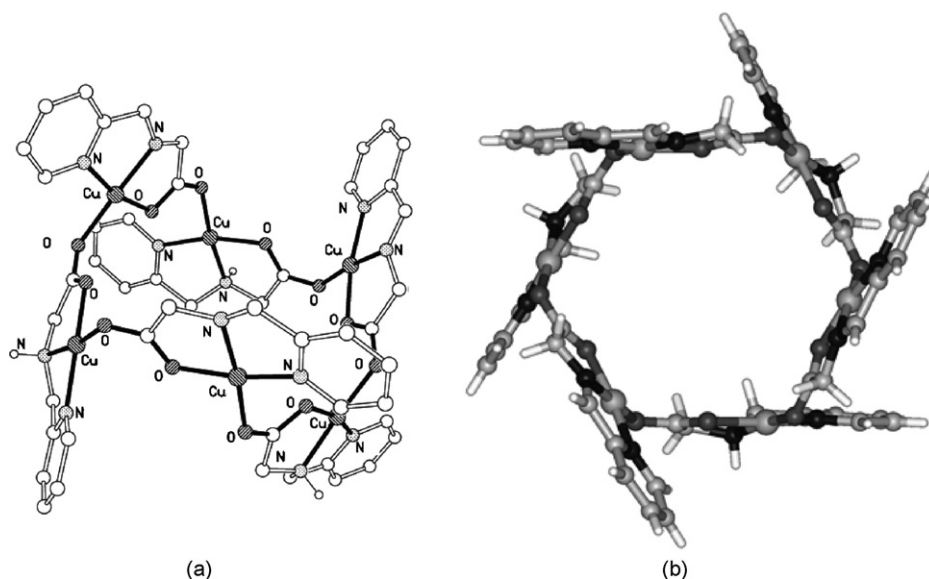


Fig. 23. (a) Cyclohexane-like crown **44**. (b) Top view showing the hexagon-shaped cavity in **44**.

anal geometry, forming two five membered rings, and the fourth position of the square planar geometry at Cu(II) is completed by the oxygen atom of the carboxylate group from the neighboring ligand. The Schiff base and the reduced Schiff base ligands are arranged alternatively in the hexanuclear cation, which has a crystallographic threefold rotational symmetry. The differences in the conformation of the backbone of the pgly and spgly ligands are clearly established from the bond distances and angles. The molecular hexamer is highly puckered in which the Cu(II) centers form a “cyclohexane-like” ring where all the Schiff base ligands are distributed on one face of the metallacyclic ring, and the pgly ligands are on the other face forming a crown. Most of the hexanuclear metallamacrocycles have their cavity filled with another metal. Such rings with no metal in the cavities are rare [26] which may be attributed to the crown-like geometry; however, the cation in **44** appears to be the first molecular hexamer containing mixed ligands.

The reaction between Hpgly.HCl and $\text{Cu}(\text{ClO}_4)_2 \cdot 6\text{H}_2\text{O}$ yielded $[\text{Cu}(\text{pgly})(\text{H}_2\text{O})]\text{ClO}_4$ (**45**) instead of the expected cyclic oligomer [24], although the stoichiometric ratio of the ligand to metal is the same as used in the synthesis of **44**. Unfortunately, no crystal structure is available for **45**; however, the difference between $\nu_{\text{as}}(\text{CO}_2^-)$ and $\nu_{\text{s}}(\text{CO}_2^-)$ in the IR spectrum has been successfully used to derive information regarding bonding modes of carboxylate anions [27]. The $\Delta\nu$ of 178 cm^{-1} indicated the bridging mode of the carboxylate group in **45**. On the basis of this information, the structure of **45** may be presumed to be a 1D polymer rather than a monomer. Further, the electrospray ionization mass spectrometry (ESI-MS) has been used to distinguish **44** from **45**. The isolation of metallamacrocyclic cation **45** depends on the nature of the reactants. Such dependency is unusual in metallasupramolecular chemistry.

4.3. Influence of anions on 1D polymers

1D coordination polymers are the most commonly encountered species. Non-coordinating as well as coordinating counter anions play an important role in the formation of such supramolecular structures. Compared to the non-coordinating anions, the coordinating anions have more impact on the polymeric structures, especially when the latter can also act as a bridging ligand in addition to participating in metal coordination. Sometimes, these anions can also help in hosting the water chains *via* hydrogen bonding. In this section, the effect of some common anions on the conformation of 1D coordination polymers is described.

Reaction of CuCl_2 with pgly and pala gives $[\text{Cu}(\text{pgly})\text{Cl}] \cdot \text{H}_2\text{O}$ (**46**) and $[\text{Cu}(\text{pala})\text{Cl}] \cdot \text{H}_2\text{O}$ (**47**), respectively [28]. In both the cases Cu(II) complexes have infinite 1D coordination polymeric structures with zigzag conformation through unsymmetrical Cl–Cu–Cl bridging and sustained by $\text{N–H} \cdots \text{O}=\text{C}$ interactions. These chains are further linked together through weak $\text{C–H} \cdots \text{Cl}$ interactions. Hydrogen-bonded single stranded water chains have been hosted by the hydrophilic channels provided by the carbonyl groups in the crystal packing as shown in Fig. 24.

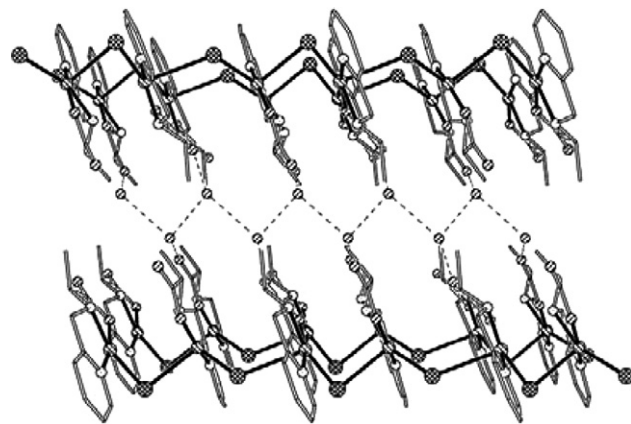


Fig. 24. Packing of single-stranded water chain in the hydrophilic pockets of **47**.

In $[\text{Cu}(\text{pala})(\text{CH}_3\text{COO})] \cdot 0.75\text{H}_2\text{O}$ (**48**) the pala ligand has *mer* conformation and occupies the equatorial positions of the square base [28]. The apical and the fourth equatorial positions of Cu(II) are occupied by oxygen atoms of two bridging acetate ligands to generate 1D $\Delta\Delta\Delta\Delta$ spiral coordination polymeric chains which are aligned parallel and held together by strong $\text{N–H} \cdots \text{OH}_2$ hydrogen bonds. This spiral coordination polymeric structure does not have water chains; instead it has a single water molecule hydrogen bonded to the metal complex. The NO_3^- anion in $[\text{Zn}(\text{pgly})(\text{NO}_3)]$ (**49**) coordinates Zn(II) as a monodentate ligand and is not able to compete with the carbonyl oxygen of the pala ligand in the bridging ability to produce a zigzag 1D polymer [28] sustained by hydrogen bonds as shown in Fig. 25. Such carbonyl oxygen bridging has usually led to the formation of helical structures [29].

Colorless crystals of $[\text{Pb}(\text{pala})(\text{ClO}_4)]_n$ (**50**) were obtained when pala anion reacted with Pb(II) perchlorate [30]. In the solid-state structure all the potential binding sites of the pala ligand have been utilized. The Pb(II) atom is strongly bonded

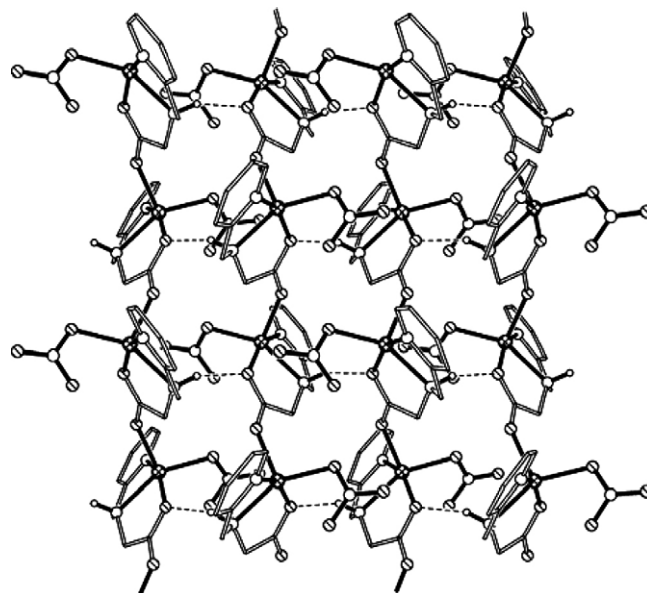


Fig. 25. A portion of the packing diagram of **49**.

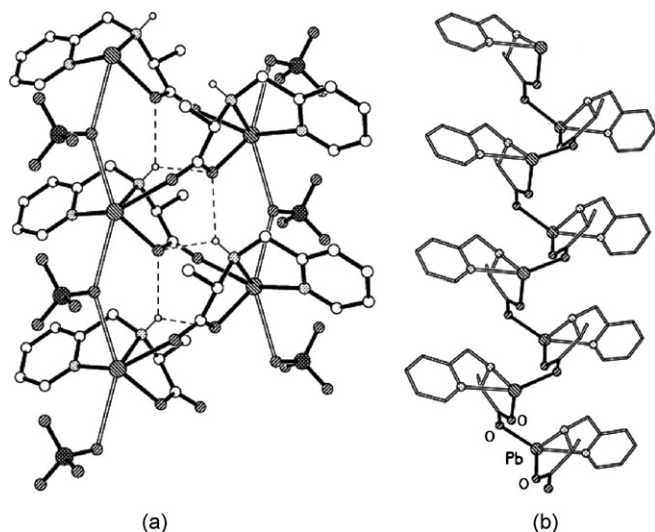


Fig. 26. (a) A Diagram showing the inter-strand interactions between helical coordination chains of **50** and (b) a portion of the helical chain.

to the two N and one O atom of the same pala ligand and a carbonyl oxygen of the neighboring ligand to yield a distorted trigonal pyramidal geometry. The bonding between Pb(II) and the neighboring carbonyl oxygen atom generates a 1D helical polymer (Fig. 26a). The right-handed helical polymers are all arranged parallel to the 2_1 screw axis with a pitch of 5.59 Å (equal to the unit cell length, a) as shown in Fig. 26b. The shape of the helical chain is oval with approximate dimensions 2.26 (O...O) and 4.27 (Pb...Pb) Å in the bc plane. The helical polymers are further stabilized by bridging ClO₄⁻ anions and very weak N–H...O hydrogen bonds ($D_{H...O}$ 2.42 and 2.60 Å). If the Pb...O...Pb interactions from perchlorate anions are included then the structure may well be described as a pillared-helical structure. The corresponding nitrate derivative is also presumed to have a similar helical structure with Pb...O(of nitrate)...Pb scaffolding in the solid state.

4.4. Solvent dependent supramolecular assembly

As discussed earlier, the isolation of coordination polymeric compounds with different connectivity pattern depends on various factors, including the stoichiometry of the reactants, pH and counter ions etc. The formation of supramolecular structures also depends on the nature of solvents used. For instance, the conversion of the metallacrown cation, [K(ClO₄)₃Cu₃(pala)₃]⁺, into a 1D coordination polymer, [Cu(pala)(H₂O)]_{*n*}^{*n*+} discussed below, has been found to be water dependent.

The reaction of Cu(ClO₄)₂·6H₂O with Hpala and KOH in equimolar ratio in MeOH–MeCN gives a potassium-ion incorporated tricopper metallamacrocyclic compound, [K(ClO₄)₃Cu₃(pala)₃](ClO₄) (**51**) [24]. The basic unit of the cation consists of a trimer formed by cyclization of Cu(pala) moieties where the pala ligand is coordinated to Cu(II) in a *mer* geometry. The exogenous oxygen of the carboxylate group in the pala ligand is intramolecularly bonded to the fourth position of the square base of the next Cu(II) to provide a N₂O₂ donor set to the metal atom. The Cu₃(pala)₃ trimer has

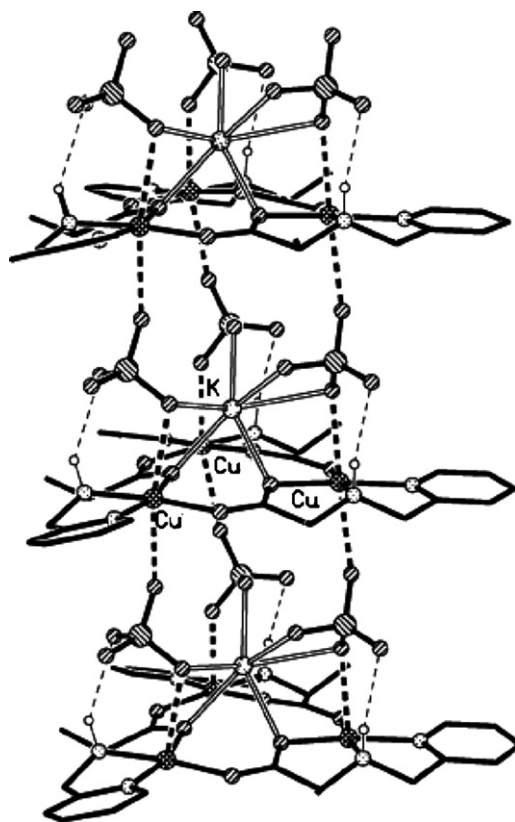
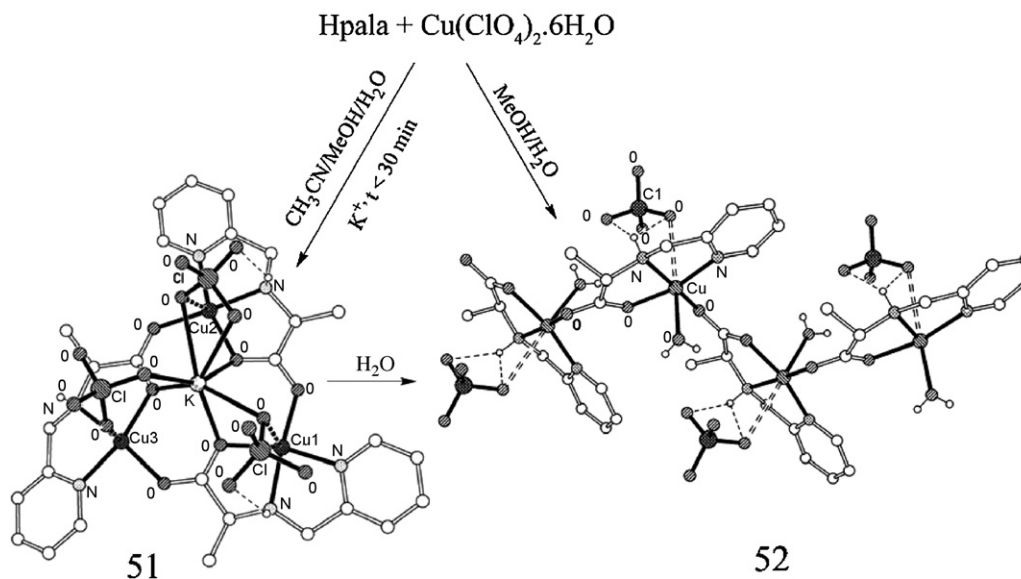


Fig. 27. A view of the packing of metallamacrocycle, **51**, in the solid-state.

an approximate noncrystallographic C_3 symmetry, with all the N–H protons on one side of the Cu₃ plane. A K⁺ ion is found above the Cu₃ plane by 1.897 Å and bonded to three oxygen atoms of the [Cu₃(pala)₃]³⁺ cation. The highly distorted pentagonal bipyramidal coordination geometry at K⁺ ion is completed by the oxygen atoms of three ClO₄⁻ ions. The three perchlorate ions further interact with the trimer through Cu...OClO₃ bonds and medium N–H...O hydrogen bonds. In the solid-state structure, these [K(ClO₄)₃Cu₃(pala)₃]⁺ units pack through weak Cu–O_{axial} bonding from the perchlorate oxygen atoms to form an infinite 1D polymeric structure as shown in Fig. 27. In other words, [K(ClO₄)₃]²⁻ units are sandwiched between [Cu₃(pala)₃]³⁺ alternatively. The Cu–O_{axial} distances are in the range 2.43(1)–2.58(1) Å. One non-coordinating ClO₄⁻ ion has been found to fill the empty space in the lattice.

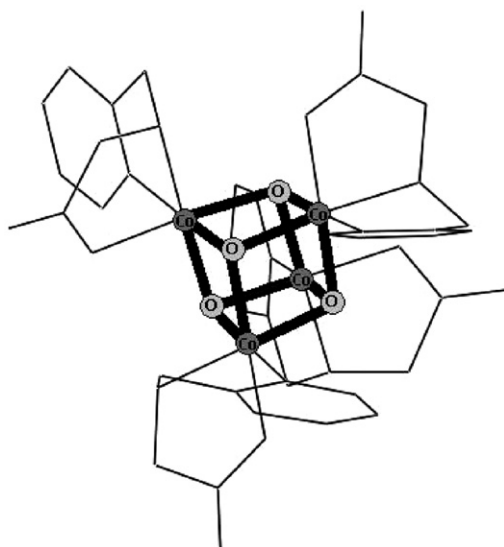
When the same reaction was repeated in the absence of the K⁺ ion in water, a 1D coordination polymeric compound, [Cu(pala)(H₂O)]ClO₄ (**52**), resulted as the only isolable product in moderate yield [24]. Further, two oxygen atoms of the ClO₄⁻ anion are involved in weak N–H...O hydrogen bonding to the N–H proton ($d_{O...H}$, 2.48(2) and 2.54(2) Å) which accounts for the highly ordered behavior of this anion in the crystal lattice. It is interesting to note that dark blue **51** crystallized as a major product from MeCN–MeOH–H₂O solution after only 10 min of stirring. Prolonged stirring of the reaction mixture resulted in the formation of **52**. It has been found that **52** is exclusively formed in the aqueous solution, and the potassium ion has no influence on the formation of final product, **52**. It is one of the exam-

Fig. 28. Solvent dependent formation of **51** and **52**.

ples of solvent-dependent formation of supramolecular species as depicted in Fig. 28.

4.5. Formation of cubane-like aggregate

Reaction of CoCl₂·6H₂O with Hpgly in the presence of KOH followed by oxidation with PbO₂ leads to the formation of a tetranuclear cobalt(III) complex with the cubane Co₄O₄ core, [Co₄(pgly)₄(μ₃-O)₄] (**53**) (see Fig. 29) [31]. This complex has four N–H···O intramolecular hydrogen-bonds between the amino group on one of the four cobalt atoms and the carboxylate group on another cobalt atom. The four-membered rings, Co–μ₃-O–Co–μ₃-O, are approximately planar. The Co–μ₃-O–Co angles (93.8–97.3°) and the μ₃-O–Co–μ₃-O angles (82.5–85.1°) are larger and smaller than the right angle,

Fig. 29. Cubane-like structure of **53**.

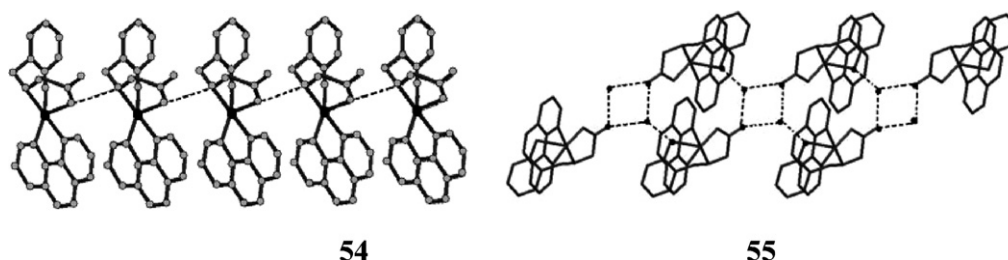
respectively. The non-bonding Co–Co distances are in the range of 2.77–2.87 Å.

5. Ternary complexes

Although Sgly, Sala and Sbal anions are very good tridentate ligands, in the presence of a co-ligand such as 2,2'-bipyridine (2,2'-bpy), 4,4'-bipyridine (4,4'-bpy) or 1,10-phenanthroline (phen), the phenolato oxygen atoms of these tridentate ligands may be protonated and/or freed from the metal centre depending on the pH of the solution employed. Thus they can act as bidentate ligands, especially for Cu(II), leading to the formation of 2D or 3D frameworks. However, the uncoordinated phenolic O atom has a choice concerning intermolecular hydrogen bonding. In order to further understand the coordination behavior of the reduced Schiff bases in the presence of the above mentioned nitrogen containing co-ligands, the ternary Cu(II) complexes of H₂Sgly, H₂Sala and H₂Sbal ligands have been studied. The important structural features are highlighted below.

5.1. Complexes with 1,10-phenanthroline as co-ligand

Reaction of phen and H₂Sgly, with Cu(CH₃COO)₂·H₂O or Cu(ClO₄)₂·6H₂O in an equimolar ratio gives [Cu(Sgly)(phen)]·2.75H₂O (**54**) and [Cu(HSgly)(phen)]ClO₄·1.5H₂O (**55**), respectively [32]. In the presence of the phen co-ligand the phenolic oxygen of the reduced Schiff base does not participate in bridging. The monomeric units of **54** are held together by intermolecular hydrogen bonding involving amine-H and carboxylate O atoms to form a 1D hydrogen-bonded polymer. Monoprotonation of the ligand in **55** changed the coordination environment and the conformation of the ligand at the metal center as shown in Fig. 30. The phenolic ring is nearly aligned parallel to the phen ligand and

Fig. 30. Packing of **54** and **55** through supramolecular interactions.

perpendicular to the carboxylate group. Due to $\pi \cdots \pi$ interaction between the phenolate ring and phen, a shorter distance than normal between Cu(II) and phenolic O is observed. Both the protons of the lattice water are involved in strong hydrogen bonding with the protonated phenolic group to give a 1D polymer.

The crystal structure of $[\text{Cu}(\text{HSala})(\text{phen})]\text{ClO}_4 \cdot 0.625\text{H}_2\text{O}$ (**56**), is very similar to **55** and also shows intramolecular stacking between coordinated phen and the phenolic ring of the ligand [32]. But unlike **55**, in **56** the perchlorate anions are not disordered owing to the strong $\text{O}-\text{H} \cdots \text{O}$ and $\text{N}-\text{H} \cdots \text{O}$ hydrogen bonds to the phenolic and N-H protons.

When the co-ligand is added in more than the equimolar ratio, $[(\text{phen})\text{Cu}(\mu\text{-Sgly})\text{Cu}(\text{phen})_2](\text{ClO}_4)_2 \cdot 3\text{H}_2\text{O}$ (**57**), is obtained [33] containing a dinuclear cation in which the $[\text{Cu}(\text{Sgly})\text{phen}]$ moiety is bonded to the $[\text{Cu}(\text{phen})_2]^{2+}$ cation through an oxygen atom of the carboxylate group of the ligand. Except for the conformation of the ligand backbone, the $[\text{Cu}(\text{Sgly})\text{phen}]$ moiety is very similar to **55**; $\pi \cdots \pi$ interactions between two parallel phen ligands from the neighboring unit is observed in the solid state. The conversion between the neutral, **55**, and

protonated complex, **57** (as shown in Fig. 31) was also investigated. UV-vis spectral titration indicates the reversibility of protonation in solution [33].

From a reaction mixture containing $\text{Cu}(\text{ClO}_4)_2 \cdot 6\text{H}_2\text{O}$, phen, *N*-(2-hydroxybenzyl)- β -alanine (H_2Sbal) and LiOH in the ratio of 1:1:1:1, a 1D coordination polymer $[\text{Cu}_3(\text{Sbal})_2(\text{phen})(\text{H}_2\text{O})_2](\text{ClO}_4)_2 \cdot 3\text{H}_2\text{O}$ (**58**) and a hydrogen-bonded 1D chain $[\text{Cu}(\text{H}_2\text{Sbal})_2(\text{phen})](\text{ClO}_4)_2$ (**59**) were isolated in successive steps. When the ratio of the base was doubled, the neutral monomer, $[\text{Cu}(\text{Sbal})(\text{phen})] \cdot 2\text{H}_2\text{O}$ (**60**) was obtained. Addition of HClO_4 to **60** furnished **58** and **59**, and this mixture can be converted back to **60** by the addition of a base. This conversion of monomer to two 1D-polymers was found to be reversible [33]. This conversion is schematically displayed in Fig. 32.

The fragments $[\text{Cu}_2(\text{Sbal})_2(\text{H}_2\text{O})_2]$ and $[\text{Cu}(\text{phen})]^+$ are the building blocks of the 1D polymeric cation $[\text{Cu}_3(\text{Sbal})_2(\text{phen})(\text{H}_2\text{O})_2]\text{ClO}_4 \cdot 3\text{H}_2\text{O}$ (**58**). Two tridentate dianionic ligands with bridging phenolate groups form the basal plane of the distorted square pyramidal geometry of the two Cu(II) centers of the dimer and the fifth apical position is occupied by water. The two “free” carbonyl groups of the ligand further link the

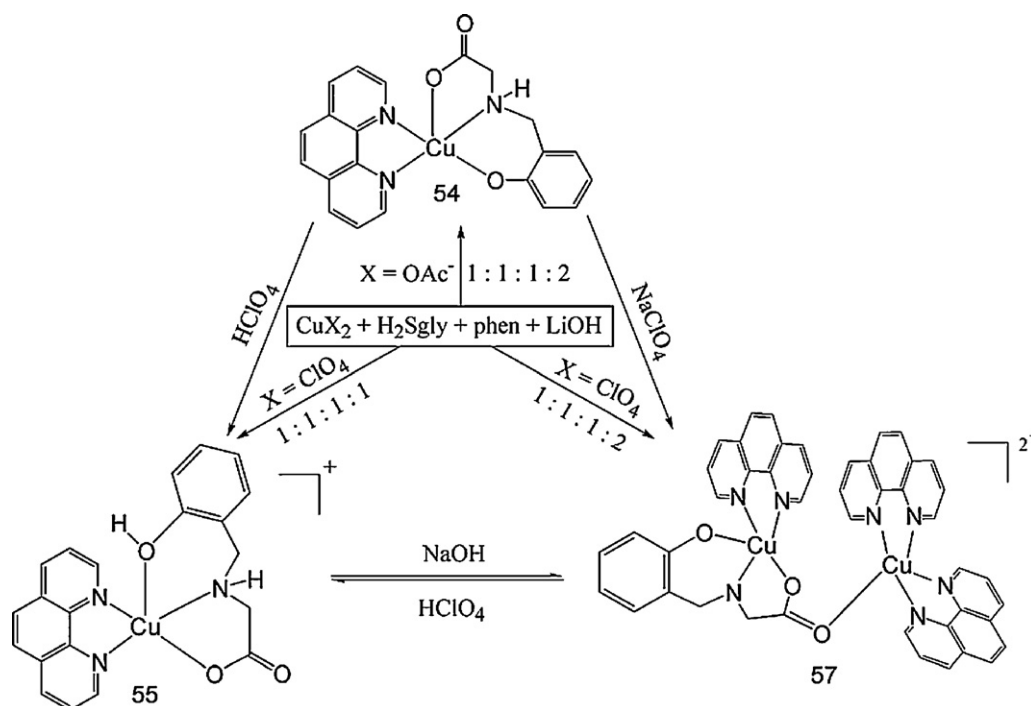
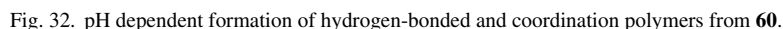


Fig. 31. A scheme showing the interconversion of monomeric structures due to protonation.



The presence of two lattice water molecules in **60** generates an interesting solid-state structure and the 1D zigzag water chain, as shown in Fig. 33, is sustained by hydrogen bonding to the uncoordinated carbonyl oxygen atoms.

Though $[\text{Cu}(\text{H}_2\text{SbAl}_4)_2(\text{phen})](\text{ClO}_4)_2$ (**61**) [34] has connectivity very similar to that of **59**, the conformation of the ligand backbone is different. Moreover, the $\text{N}-\text{H} \cdots \text{O}$ bonding pattern is also different, with the phenolic protons being bonded to anions. In the dimer $[\text{Cu}_2(\text{Sbal})(\text{phen})_3](\text{NO}_3)_2 \cdot 2.5\text{H}_2\text{O}$ (**62**) monomer $[\text{Cu}(\text{Sbal})(\text{phen})]$ is bonded to the cation $[\text{Cu}(\text{phen})_2]^+$ through the oxygen atom of the delocalized carboxylate group of the ligand. Though the geometric parameters of the $[\text{Cu}(\text{Sbal})(\text{phen})]$ fragment are similar to **59**, the conformation of the ligand backbone is different. Unlike in **59**, where the phenolic aromatic ring

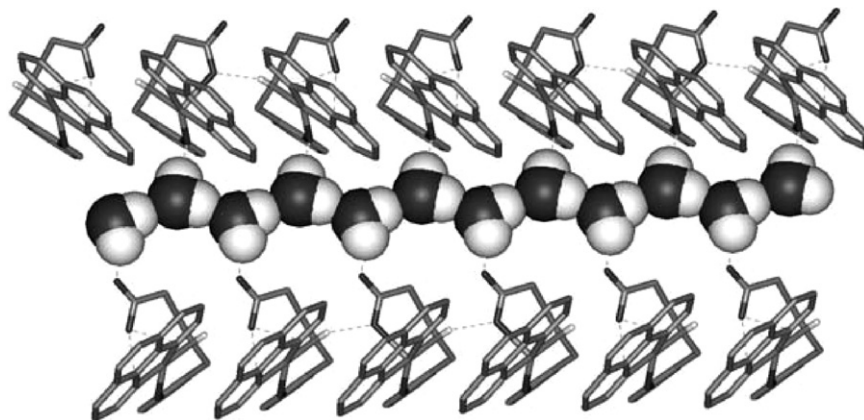


Fig. 33. Hydrogen-bonded 1D water chain hosted by **60**.

is nearly in a plane with the phen ligand, in **62**, it is perpendicular to phen. The two phen ligands are bent towards each other with an interplanar angle of 15.2° , showing the presence of strong $\pi \cdots \pi$ interactions. $[\text{Cu}_2(\text{Sab4})(\text{phen})_3](\text{ClO}_4)_2 \cdot 3\text{H}_2\text{O}$ (**63**) has structure similar to **62**.

An interesting 3D hydrogen-bonding network is generated by the five water molecules present in the zwitterion $[\text{Cu}(\text{Sab4})(\text{phen})(\text{H}_2\text{O})] \cdot 5\text{H}_2\text{O}$ (**64**). In the mononuclear unit Cu(II) has a square pyramidal geometry with a N_3O_2 donor set but the fifth apical site is not occupied by the carboxylate oxygen but by the aqua ligand. Complementary $\text{N}-\text{H} \cdots \text{O}=\text{C}$ hydrogen bonds are present between pairs of **64** complexes. Second complementary $\text{O}-\text{H} \cdots \text{O}$ bonding between the phenolic O and one of the hydrogen atoms of the coordinated aqua ligand propagates the 1D supramolecular assembly [34] as shown in Fig. 34. The water molecules form an interesting tape-like structure.

5.2. Complexes with other co-ligands

In addition to phen, 2,2'-bpy is also a good bidentate ligand which can block the coordination sites of metal ions to allow the propagation of the polymer in a directional manner. Moreover, 4,4'-bpy, and to some extent 4-aminopyridine (4- H_2Npy), are very good rigid bridging ligands that may play an important role in extending 1D chains to generate 3D frameworks. The change in the framework caused by the introduction of a bridging ligand can give rise to product with interesting magnetic properties in the case of the coordination polymers of Cu(II).

Reaction of Cu(II) ions with H_2Sgly and H_2Sala in the presence of 2,2'-bpy gives $[\text{Cu}(2,2'\text{-bpy})(\text{HSgly})]\text{Cl} \cdot 2\text{H}_2\text{O}$ (**65**) and $[\text{Cu}(2,2'\text{-bpy})(\text{HSala})](\text{NO}_3) \cdot 2\text{H}_2\text{O}$ (**66**). Both have similar chain-like structure with Cu(II) coordinated by the 2,2'-bpy aromatic N as well as by the amine-N and carboxylate O in the basal plane [35]. The distorted octahedron is completed by phenolato O and carboxylate O from a neighboring ligand. The bridging carboxylate anion gives rise to a 1D helical coordination polymer. The only notable difference between the two structures is that, in **65** both left- and right-handed helical chains are present whereas in **66** only single-helical chains exist in the solid. No noticeable interactions were found between the strands.

A 3D chiral architecture is exhibited by $[\text{Cu}_2(4,4'\text{-bpy})_2(\text{Sala})_2] \cdot 4.5\text{H}_2\text{O}$ (**67**). A (4,4) square grid structure with an $11 \times 11 \text{ \AA}$ dimension is formed by the $[\text{Cu}(4,4'\text{-bpy})_2]^{2+}$ cation as shown in Fig. 35. In the mononuclear “anionic” fragment, $[\text{Cu}(\text{Sala})_2]^{2-}$, square planar Cu(II) has N_2O_2 donor set from the second ligand to give chirality to the fragment. The cationic and the anionic layers are connected by the carbonyl oxygen of the ligands to form a 3D supramolecular framework. The small chiral channels resulting from the weak interaction between the cation layers are filled with the water molecules [36].

The ladder shaped 1D chain is formed by the 4,4'-bpy which bridges the binuclear unit $[\text{Zn}_2(\text{Sala})_2]$ in $[\text{Zn}_2(\text{Sala})_2(4,4'\text{-bpy})] \cdot 5\text{H}_2\text{O}$ (**68**). A complicated 3D supramolecular framework is formed by the hydrogen bonds connecting each dimer unit with four other such units from different chains around it. Four binuclear units also form an eight-membered ring that is not

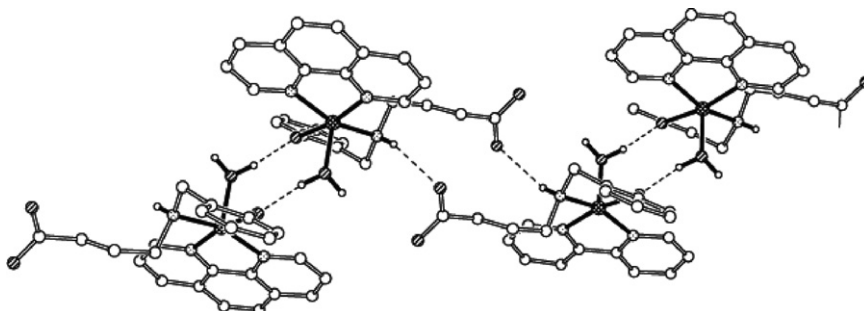


Fig. 34. A view of 1D hydrogen bonding in **64**.

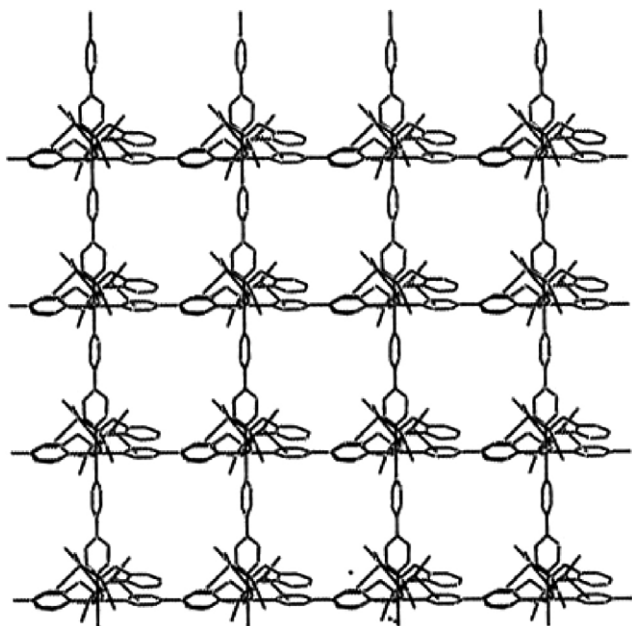


Fig. 35. The 2D grid-like layer formed by **67**.

only connected by the 4,4'-bpy but also by hydrogen bonds. In the similar complex, $[\text{Zn}_2(\text{Sala})_2(4\text{-H}_2\text{Npy})_2]\cdot 2\text{H}_2\text{O}$ (**69**) the presence of two secondary amine protons along with two uncoordinated carboxylic atoms makes it an ideal complex for extensive hydrogen bonding. Unlike **68**, in **69** the eight-membered square rings formed by the four binuclear units are held by hydrogen bonds only through $\text{N-H}\cdots\text{O}$ bonds. Both H-bond donors ($-\text{NH}_2$) and acceptors ($-\text{COOH}$) present in the eight membered ring further leads to a 2D supramolecular network by linking to each other [37].

6. Conclusions

This contribution deals with the reduced Schiff base ligands, derived from natural as well as unnatural amino acids, as a class of multidentate ligands and discusses their mode of binding and coordination to different transition metal ions such as Cu(II), Zn(II), Ni(II), etc. Several types of metallasupramolecular structures involving various metal complexes have been encountered. The supramolecular aggregates are greatly influenced by the coordination geometries around the metal centers as defined by the ligands. Further, the observed structural diversity has been attributed to the role of different donors and acceptors, aqua ligand and solvents, nature of the ligands and metal ions, coordination geometry around the metal ions and counter ions. The experimental conditions such as temperature and pH have also influenced the formation of supramolecular structures in the solid state. The influence of the hydrogen atom on the secondary amine of the reduced Schiff base ligands over azomethine ($-\text{CH}=\text{N}-$) fragment of the Schiff base is exemplified by its participation in strong hydrogen bonds ($\text{N-H}\cdots\text{O-H}$ and $\text{N-H}\cdots\text{O}=\text{C}$) that aided the construction of interesting metallasupramolecules. Apart from this, the solid-state structures revealed various $\text{C}=\text{O}\cdots\text{H}-\text{O}_{\text{solvent}}$, $\text{O-H}\cdots\text{O}$, hydrogen bonds and $\text{C}=\text{O}\cdots\pi$, $\text{C-H}\cdots\pi$, and $\pi\cdots\pi$ stacking interactions

that are further sustained by hydrogen bonds *via* the amine H-atom.

Utilization of reduced Schiff bases and fine tuning their coordination modes by modifying their structure/backbone with appropriate functional groups offers the possibility for them to be used as simple, valuable and inexpensive bricks in the construction of new supramolecular structures. It is the case that chiral metal organic frameworks of diverse topologies and functionalities can be designed *via* modular approach. Designing chiral architectures from achiral molecular compounds represents a promising theme in materials science. However, the use of simple and available chiral precursors as an alternative remains another practical approach. The facile tunability of such molecular building blocks should allow precise engineering of chiral cavities and functionalities within these chiral porous metal organic frameworks.

Besides conventional bench top synthetic methods, high temperature hydrothermal or solvothermal approach might open new avenues for making thermodynamically stable multi-dimensional coordination polymeric architectures by the judicious choice of ligands and metal ions. Finally, this review gives an insight into the understanding of the coordination chemistry of reduced Schiff base ligands in terms of various factors that should be considered for the design of coordination polymers with specific properties and functions.

Acknowledgements

This work is supported by the funds from the Ministry of Education through the National University of Singapore (Grant No. R-143-000-252-112). It is a pleasure to thank the excellent co-workers who have contributed greatly to this research; their names are given in the references.

References

- [1] (a) P.A. Vigato, S. Tamburini, *Coord. Chem. Rev.* 248 (2004) 1717, and references therein;
(b) L. Casella, M. Gullotti, *J. Am. Chem. Soc.* 103 (1981) 6338;
(c) L. Casella, M. Gullotti, G. Pacchioni, *J. Am. Chem. Soc.* 104 (1982) 2386;
(d) M.R. Wagner, F. Ann Walker, *Inorg. Chem.* 22 (1983) 3021.
- [2] (a) K. Tatsumoto, A.E. Martell, *J. Am. Chem. Soc.* 103 (1981) 6203;
(b) K. Tatsumoto, A.E. Martell, R.J. Motekaitis, *J. Am. Chem. Soc.* 103 (1981) 6197;
(c) H.M. Dawes, J.M. Waters, T.N. Waters, *Inorg. Chim. Acta* 66 (1982) 6629;
(d) I. Bkouche-Waksman, J.M. Barbe, A. Kvik, *Acta Crystallogr. B* 44 (1988) 595;
(e) R. Hamalainen, U. Turpeinen, *Acta Crystallogr. C* 41 (1985) 1726;
(f) K. Korhonen, R. Hamalainen, U. Turpeinen, *Acta Crystallogr. C* 40 (1984) 1175;
(g) K. Nakagima, M. Kojima, K. Foriumi, K. Saito, J. Fujita, *Bull. Chem. Soc. Jpn.* 62 (1989) 760;
(h) V. Kettmann, E. Fresova, *Acta Crystallogr. C* 49 (1993) 1932.
- [3] L. Casella, M. Guillotti, *Inorg. Chem.* 22 (1983) 2259.
- [4] L.L. Koh, J.D. Ranford, W.T. Robinson, J.O. Stevenson, A.L.C. Tan, D. Wu, *Inorg. Chem.* 35 (1996) 6466.
- [5] C.T. Yang, M. Vetrivelvan, X. Yang, B. Moubaraki, K.S. Murray, J.J. Vittal, *J. Chem. Soc., Dalton Trans.* (2004) 113.
- [6] X. Yang, J.D. Ranford, J.J. Vittal, *Cryst. Growth Des.* 4 (2004) 781.

- [7] J.J. Vittal, *Coord. Chem. Rev.* 251 (2007) 1781.
- [8] (a) J.D. Ranford, J.J. Vittal, D. Wu, X. Yang, *Angew. Chem. Int. Ed.* 38 (1999) 3498;
(b) X. Yang, D. Wu, J.D. Ranford, J.J. Vittal, *Cryst. Growth Des.* 5 (2005) 41;
(c) J.D. Ranford, J.J. Vittal, D. Wu, *Angew. Chem. Int. Ed.* 37 (1998) 1114.
- [9] J.X. Xu, M.Q. Chen, Z.H. Wang, H.L. Zhang, *Acta Chim. Sin.* 4 (1989) 34.
- [10] J.J. Vittal, X. Yang, *Cryst. Growth Des.* 2 (2002) 259.
- [11] B. Sreenivasulu, J.J. Vittal, *Cryst. Growth Des.* 3 (2003) 635.
- [12] B. Sreenivasulu, F. Zhao, S. Gao, J.J. Vittal, *Eur. J. Inorg. Chem.* (2006) 2656.
- [13] B.-Y. Lou, D.-Q. Yuan, L. Han, B.-L. Wu, M.-C. Hong, *Chinese J. Struct. Chem.* 24 (2005) 759.
- [14] B. Sreenivasulu, M. Vetrichelvan, F. Zhao, S. Gao, J.J. Vittal, *Eur. J. Inorg. Chem.* (2005) 4635.
- [15] (a) B.F. Hoskins, R. Robson, *J. Am. Chem. Soc.* 112 (1990) 1546;
(b) R.W. Gable, B.F. Hoskins, R. Robson, *J. Chem. Soc., Chem. Commun.* (1990) 1677;
(c) M.J. Zaworotko, *Chem. Commun.* (2001) 1;
(d) B. Moulton, M.J. Zaworotko, *Chem. Rev.* 101 (2001) 1629;
(e) A.N. Khlobystov, A.J. Blake, N.R. Champness, D.A. Lemenovskii, A.G. Majouga, N.V. Zyk, M. Schröder, *Coord. Chem. Rev.* 222 (2001) 155;
(f) B. Kumar, M. Fujita, *J. Chem. Soc., Dalton Trans.* (2000) 3805;
(g) L. Carlucci, G. Ciani, D.M. Proserpio, *New J. Chem.* 22 (1998) 1319;
(h) S.R. Batten, R. Robson, *Angew. Chem. Int. Ed.* 37 (1998) 1460;
(i) S.R. Batten, B.F. Hoskins, R. Robson, *Chem. Eur. J.* 6 (2000) 156;
(j) S.R. Batten, *Cryst. Eng. Commun.* 3 (2001) 67.
- [16] M.A. Alam, M. Nethaji, M. Ray, *Inorg. Chem.* 44 (2005) 1302.
- [17] B. Sreenivasulu, J.J. Vittal, *Angew. Chem. Int. Ed.* 43 (2004) 5769.
- [18] M. Albrecht, *Chem. Rev.* 101 (2001) 3457.
- [19] S. Khatua, S. Dasgupta, K. Biradha, M. Bhattacharjee, *Eur. J. Inorg. Chem.* (2005) 5005.
- [20] C.P. Pradeep, P.S. Zacharias, S.K. Das, *Inorg. Chem. Commun.* 9 (2006) 1071.
- [21] M.A. Alam, M. Nethaji, M. Ray, *Angew. Chem. Int. Ed.* 42 (2003) 1940.
- [22] J.J. Vittal, W. Xiaobai, J.D. Ranford, *Inorg. Chem.* 42 (2003) 3390.
- [23] (a) D.E. Fenton, in: A.F. Williams, C. Floriani, A.E. Merbach (Eds.), *Perspectives in Coordination Chemistry*, VCH Weinheim, 1992, p. 203;
(b) A. Messerschmidt, R. Ladenstein, R. Huber, M. Bolognesi, L. Avigliano, R. Petruzelli, A. Rossi, A. Finazzo-Agró, *J. Mol. Biol.* 224 (1992) 179;
(c) H. Adams, N.A. Bailey, M.J.S. Dwyer, D.E. Fenton, P.C. Hellier, P.D. Hemsstead, *J. Chem. Soc., Chem. Commun.* (1991) 1297.
- [24] X. Wang, J.J. Vittal, *Inorg. Chem.* 42 (2003) 5135.
- [25] V.R. Correia, A.J. Bortoluzzi, A. Neves, A.C. Joussef, M.G.M. Vieira, S.C. Batista, *Acta Crystallogr. E* 59 (2003) m464.
- [26] (a) N. Matsumoto, Y. Motoda, T. Matsuo, T. Nakashima, N. Re, F. Dahan, J.-P. Tuchagues, *Inorg. Chem.* 38 (1999) 1165;
(b) R.W. Saalfrank, I. Bernt, E. Uller, F. Hampel, *Angew. Chem. Int. Ed.* 36 (1997) 2482;
(c) B. Kwak, H. Rhee, S. Park, M.S. Lah, *Inorg. Chem.* 37 (1998) 3599;
(d) M. Moon, I. Kim, M.S. Lah, *Inorg. Chem.* 39 (2000) 2710.
- [27] G.B. Deacon, R.J. Phillips, *Coord. Chem. Rev.* 33 (1980) 227.
- [28] X. Wang, J.D. Ranford, J.J. Vittal, *J. Mol. Struct.* 796 (2006) 28.
- [29] (a) J.J. Vittal, in: J.J. Vittal, E.R.T. Tiekink (Eds.), *Frontiers in Crystal Engineering*, Wiley, England, 2005;
(b) S.L. James, *Chem. Soc. Rev.* 32 (2003) 276.
- [30] X. Wang, J.J. Vittal, *Inorg. Chem. Commun.* 6 (2003) 1074.
- [31] T. Ama, K.-i. Okamoto, T. Yonemura, H. Kawaguchi, A. Takeuchi, T. Yasui, *Chem. Lett.* (1997) 1189.
- [32] C.T. Yang, B. Moubaraki, K.S. Murray, J.J. Vittal, *J. Chem. Soc., Dalton Trans.* (2003) 880.
- [33] C.T. Yang, B. Moubaraki, K.S. Murray, J.D. Ranford, J.J. Vittal, *Inorg. Chem.* 40 (2001) 5934.
- [34] C.T. Yang, J.J. Vittal, *Inorg. Chim. Acta* 344 (2003) 65.
- [35] Z. Lü, D. Zhang, S. Gao, D. Zhu, *Inorg. Chem. Commun.* 8 (2005) 746.
- [36] B.-Y. Lou, D.-Q. Yuan, S.-Gao, Y. Xu, R.-H. Wang, Y. Xu, L. Ham, M.-C. Hong, *J. Mol. Struct.* 707 (2004) 231.
- [37] B.-Y. Lou, D.-Q. Yuan, B.-Y. Lou, R.-H. Wang, Y. Xu, B.-L. Wu, L. Ham, M.-C. Hong, *J. Mol. Struct.* 698 (2004) 87.